

Florida State University Libraries

Electronic Theses, Treatises and Dissertations

The Graduate School

2013

Pleistocene Calcareous Nannofossil Biostratigraphy of Site U1352, Canterbury Basin, New Zealand

Nicholas R. Myers



THE FLORIDA STATE UNIVERSITY
COLLEGE OF ARTS AND SCIENCES

PLEISTOCENE CALCAREOUS NANNOFOSSIL BIOSTRATIGRAPHY OF SITE U1352,
CANTERBURY BASIN, NEW ZEALAND

By

NICHOLAS R. MYERS

A Thesis submitted to the
Department of Earth, Ocean and Atmospheric Sciences
in partial fulfillment of the
requirements for the degree of
Master of Science

Degree Awarded:
Spring Semester, 2013

Nicholas Myers defended this thesis on March 29, 2013.

The members of the supervisory committee were:

Sherwood W. Wise
Professor Directing Thesis

William Parker
Professor Co-Directing Thesis

Yang Wang
Professor Co-Directing Thesis

The Graduate School has verified and approved the above-named committee members, and certifies that the thesis has been approved in accordance with university requirements.

To my mother, without whom my second chance would not be possible

ACKNOWLEDGEMENTS

There have been so many individuals who have influenced my academic career here at Florida State; almost too numerous to name. The guidance and encouragement of Dr. Sherwood “Woody” Wise during this long, arduous process has been most comforting for me. The opportunities he has provided me through my graduate career, including my long tenure working at the Antarctic Marine Geology Research Facility, numerous out-of-town conferences, and research voyages in the Gulf of Mexico analyzing aspects of the BP oil spill, remain the most powerful experiences I have had during my studies here. His patience for me and this project has been second-to-none. He has been a great mentor, challenging professor, and good friend. My future endeavors will be attributed directly to the education and opportunities he has provided me during my tenure at FSU.

Special gratitude goes out to Dr. William Parker and Dr. Yang Wang, two outstanding professors of this department. Their advice, leadership and their dedication to education made students like me look forward to their classes and enjoy the experience of learning. Their assistance in the development of this document are highly appreciated.

Samples and supplemental materials for this project were graciously provided by Dr. Stacie Blair from her participation as a nannofossil paleontologist on IODP Leg 317 in 2009. Her willingness, despite her busy post-graduate schedule, to discuss taxonomy and provide insight and guidance towards the direction of this project has proven invaluable. I look forward to continuing our work together as we conduct future work on these Leg 317 nannofossils.

Dr. Denise Kulhanek, a wonderful mentor and friend, gave me tremendous assistance while I was attempting to get this project off the ground. Helping me get organized and even taking the time to Skype with me, all the way from New Zealand, shows your dedication and willingness to help others who follow in your footsteps. Thank you for all you have done for me, during my undergraduate and graduate years.

During my graduate career, I have had the pleasure of developing a wonderful camaraderie with fellow graduate students of the EOAS and nannofossil laboratory. Jen Coor, Marie Peterson, Aisha Agbali, Mohammad Aljahdali, Aaron Avery, Jarrett Cruz, and countless others have been dear friends throughout this journey, and have been here with me from the beginning. They have always been available to lend a helping hand, give a suggestion, or just

chat as we take our minds off the hustle and bustle of a busy day. My experience here would not have been as memorable without you.

My time at Florida State would not have been the same without my 5-year tenure at the Antarctic Research Facility. Dr. Charlotte Sjunneskog and Steve Petrushak have been incredible supervisors over the years, and true friends. Due to your willingness to give encouraging words and insight, your continued support made working in the ARF more than an occupation. Rather, you created a welcoming environment facilitative to learning and exploring new ideas and concepts and a job that I truly enjoyed. Special thanks to all the students and coworkers I have grown to work with and cherish. Thanks for making work so much fun!

A huge sense of appreciation goes out to the staff of the EOAS Department, Sharon Wynn, Diane Grubbs, and Michaela Lupiani, for handling my numerous questions with a sense of concern and a genuine smile. I'd also like to thank my family, Rae and Chris Myers, for your well wishes, and my friends who have been there to support me all along. Adam (AJ) Jones and Fairuz Amin have become two of the closest friends I could ask for. Special gratitude is paid to Angela Silva, a woman who has captured my heart and helped keep me on track. Thank you for all those long nights of studying and for your love and understanding while I dedicated my time and efforts to this project. Thanks to you, I can now see the finish line.

Most importantly, I'd like to thank my mother. My academic accomplishments, experiences, and future successes are a direct result of your willingness to raise me the right way and show your love and support through the roughest of times. There are no words to express how much you've meant to me. Thank you!

TABLE OF CONTENTS

List of Tables	vii
List of Figures	viii
List of Plates	ix
Abstract.....	x
1. INTRODUCTION	1
Calcareous Nannoplankton.....	1
Biostratigraphic Utility.....	2
Locality.....	4
IODP Leg 317.....	6
Site U1352.....	8
Hole U1352B.....	9
Objectives	9
2. MATERIALS AND METHODS.....	11
3. RESULTS	13
Abundance and Preservation	13
Species Evenness, Richness and Diversity Indices	13
Biostratigraphy	14
4. DISCUSSION	21
Calcareous Nannofossil Datums.....	21
Sequence Boundaries.....	22
5. SUMMARY AND CONCLUSIONS	24
APPENDICES	25
A. TAXONOMIC LIST	25
B. TABLES	27
C. FIGURES	47
D. PLATES	53
REFERENCES	55
BIOGRAPHICAL SKETCH	59

LIST OF TABLES

1	Calcareous nannofossil datums and ages in Hole U1352B	25
2	Age constraints of observed sequence boundaries in Hole U1352B derived from calcareous nannofossil age datums	26
3	Pleistocene relative calcareous nannofossil abundance in Hole U1352B	27
4	Raw semi-quantitative calcareous nannofossil abundance counts from Hole U1352B	35

LIST OF FIGURES

- | | | |
|---|---|----|
| 1 | Map of Canterbury Basin on the eastern margin of South Island, New Zealand. Primary drilling sites are indicated in red, secondary drilling sites are indicated in yellow (modified from Expedition 317 Scientists, 2010)..... | 45 |
| 2 | Regional map of New Zealand including the Otago and Banks Peninsulas (mid-Miocene volcanic centers) and Alpine Fault. | 46 |
| 3 | Correlation of lithologic units defined at slope Site U1352 and interpreted dip-oriented seismic profile. A. Uninterrupted profile showing site location. B. Sequence boundary interpretation (Expedition 317 Scientists, 2010). | 47 |
| 4 | Summary of core recovery at Site U1352. MP = Marshall Paraconformity (modified from Expedition 317 Scientists, 2010). | 48 |
| 5 | Line graph displaying the inverse relationship between Hole U1352B species richness, evenness, Shannon Diversity and abundance of <i>Gephyrocapsa aperta</i> . GREEN delineates Shannon diversity values, the BLACK graph shows species richness, species evenness is plotted in BLUE and the RED line graph represents <i>G. aperta</i> abundance. | 49 |
| 6 | Age vs. Depth Plot of observed calcareous nannofossil datums from Hole U1352B. | 50 |

LIST OF PLATES

- 1,2 Cross-Polarized Micrographs of Pleistocene calcareous nannofossils 41

ABSTRACT

IODP Leg 317 off the east coast of New Zealand cored Pleistocene strata at Site U1352 on the continental shelf over the Canterbury Basin. Shipboard biostratigraphic interpretations tend to be rough estimations due to several factors, including high drilling rates that restrict sample analysis times, therefore a shore-based refinement of the nannofossil biostratigraphy is a necessary complement to shipboard analysis. The shore-based analysis of Hole U1352B samples presented here yielded 10 biozones/zonal groups defined by 12 nannofossil datums. Of these datums, seven first occurrences (FO), four last occurrences (LO), and one first occurrence acme (FO acme) were observed; six of them were recognized via size differentiation.

Age constraints were established for six sequence boundaries observed within the sediment column that correlate well with the shipboard biostratigraphic constraints. Species richness varies greatly (six to 22 species), but were noticeably below average around predicted sequence boundaries. Species evenness and diversity display an unusual inverse relationship with *Gephyrocapsa aperta* abundance values that reflects its dominance among the other taxa in the assemblage.

Further analysis of reworked nannofossils at Site U1352 will be compared in the future with those for the slope sites (U1351, U1353, U1354). This will provide a better understanding of transport mechanisms and sediment sourcing in the Canterbury Basin depositional environment.

CHAPTER ONE

INTRODUCTION

Calcareous Nannoplankton

Coccolithophorids belong to the phylum Haptophyta that comprises golden-brown algae possessing two flagella and a flagella-like structure known as a haptonema, the purpose of which is uncertain. It may function as an aid in motility, attachment, prey capture or nutrient extraction (Inouye and Kawachi, 1994, Pienaar, 1994). These unicellular, photosynthetic, strictly marine organisms are found within the photic zone (upper 200 m of the water column), excrete calcified scales, known as coccoliths that are exclusive to haptophytes. Reproduction among this group occurs either asexually by binary fission (mitosis) or sexually via meiosis (Bown, 1998). The term “Calcareous nannoplankton” refers to their small (~10-100 μm) cell size and calcitic plates (coccoliths) that cover the cell. “Calcareous nannofossil” is the term used when referring to the extinct forms, and these are the fossilized remains of coccolithophorids within the sediment record. “Calcareous nannoplankton” refers to extant forms.

Three groups of coccoliths exist for coccolithophorids; heterococcoliths, holococcoliths, and nannoliths, and each are linked to the organism’s life stages. Heterococcoliths, usually circular to elliptical discs or rings, are composed of calcite crystals of varying sizes and shapes. According to Manton and Leedale (1969), heterococcoliths biomineralization is intracellular. These forms are most commonly associated with the diploid stages of the organisms’ lifecycle in which the primary mode of reproduction is simple mitosis. Holococcoliths, characteristically disc- or dome-shaped, differ in that they are constructed of identical, equidimensional, minute ($<0.1\mu\text{m}$) crystals and their biomineralization occurs outside of the cell (Rowson et al, 1986). Also, because that the primary mode of reproduction in holococcoliths is presumably meiotic

division, they are most often correlative to the haploid stage (Billard, 1994). Rarity of extant holococcoliths as well as in the fossil record leads to the belief that they are more susceptible to destruction (Siesser and Winter, 1994). The third group, nannoliths, is heterogeneous and comprised of a wide range of shapes, but their relationship to the coccolithophorid lifecycle is uncertain (Bown, 1998).

Although no definitive function of the coccoliths has been determined, theoretical uses have been developed. Herbivorous zooplankton feed heavily on nannoplankton, therefore coccoliths may be used as protection against, among other things, predation, although no distinct evidence has yet been discovered (Bown, 1998). Other theories towards coccolith utilization include 1) floatation and buoyancy that could allow the organism to maintain a favorable position within the photic zone, 2) reflection of light for organisms living near the surface where UV radiation is high, 3) refraction of light for organisms living in the nutrient-rich bottom waters of the photic zone to allow for more efficient capture of light (Gartner and Bukry, 1969), or 4), as originally hypothesized by Isenberg et al. (1967), coccoliths may be the by-products from the detoxification of carbonate through the fixation of calcium.

Biostratigraphic Utility

Nannofossils are particularly good for biostratigraphic studies due to their high abundance, as well as their planktonic, rapidly evolving, and largely cosmopolitan nature (Bown, 1998). They are found to be largely ubiquitous and are readily found in pelagic sediments where dissolution has impacted other calcitic microfossils. Also, their small size and large abundance within pelagic sediments provides for simple sample preparation techniques for use for research, scientific drilling, or petroleum exploration.

It was initially through the work of Bramlette and Riedel (1954) that the potential of calcareous nannofossils for use in global stratigraphic correlation was realized and early biostratigraphic frameworks were developed during 1960's. Frameworks of Bramlette and Wilcoxon (1967) and Hay et al. (1967) were established for the Cenozoic, and with the onset of scientific drilling by the Deep Sea Drilling Project (DSDP) nannofossils became a key tool in biostratigraphic correlation and paleoecological interpretation (Wise, 1982). Martini (1971) published the first "standard" nannofossil zonation scheme and subsequent research by Bukry (1973), Okada and Bukry (1980), and a plethora of others further refined the Cenozoic zonation. Mesozoic zonations made sporadic progress during the 1960's and 1970's prior to Sissingh (1977)'s production of the first all-inclusive Mesozoic zonation scheme that was accompanied by that of Roth (1978) a year later. Further refinements and compilations have been presented in publications such as Perch Nielsen (1985a,b) and Bown (1998).

Although coccolithophores provide an excellent method for stratigraphic correlation and paleoecology studies, Wise (1982) indicates several complexities that often arise with nannofossil utilization. As previously mentioned, each coccolithophore has multiple lifestages with specific coccoliths associated with each. Dimorphism refers to the phenomenon of two separate coccoliths deriving from a single cell and due to this, some species concepts may become skewed. Several species have been documented as producing multiple different sizes and shapes of coccoliths within their lifecycle, providing the means for the classification of a single species into several. Along with this issue, many calcareous objects seen in the sedimentary record have no modern equivalents, i.e. *Discoasters*, and can provide difficulties for taxonomists and biostratigraphers alike. Another major factor that can hinder nannofossil identification and utilization is diagenesis. Honjo (1976) noted that coccoliths are most effectively deposited on the

ocean floor via fecal pellets of the zooplankton inhabiting the photic zone. While this method provides a swift passage to the sediments below, dissolution below the calcite compensation depth (CCD) within the undersaturated waters of the deep ocean does occur at times and impacts the appearance of coccoliths. Upon burial in the sediments, reprecipitation of dissolved calcite onto particular forms also may hinder their identification.

Locality

The New Zealand Plateau, underlying the onshore Canterbury Plains and offshore Canterbury Basin (Field and Browne, 1989) located along the eastern margin of the southern island of New Zealand (Fig. 1), is a continental fragment that began rifting from Antarctica ~80 Ma and continued through the early Eocene (~55 Ma). The resulting spreading ridge was then truncated in the late Eocene by the linking of the Indian Ocean and Pacific spreading ridges in the southern Tasman Sea. This led to the formation of the modern plate boundary separating the Australian and Pacific plates that include the Macquarie Ridge, the Tonga-Kermadec subduction zone, and an onshore expression of the plate boundary termed the Alpine Fault (Molnar et al., 1975).

Canterbury Basin comprised part of a simple passive margin until tectonic convergence of the Australian and Pacific plates influenced the region, forming the Alpine Fault (Wellman, 1971; King, 2000) which has ~500km of total displacement since its inception ~23 Ma(Kamp, 1987). The basin is bounded to the north and south by the Otago and Banks Peninsulas, respectively, which are mid-to-late Miocene volcanic centers (Fig. 2). Basin sediments thin out towards each of these features and to the west where they onlap onshore basement rock. This basement rock was uplifted and faulted during the current phase of mountain building along the Southern Alps beginning in the late Miocene (Adams, 1979; Tippett and Kamp, 1993a; Batt et

al., 2000). The sediments of the basin represent a first-order (~80 m.y.) transgressive-regressive cycle and record the plate tectonic history of the New Zealand Plateau (Carter and Norris, 1976; Field and Browne, 1989).

The postrift transgressive phase (Onekakara Group) of this marine sedimentary section is the result of a reduction in terrigenous input, during which flooding of the land reached a maximum (Fleming, 1962), leading to the deposition of widespread calcareous biopelagites (Amuri Formation) that range in age to the early Oligocene (~33 Ma). Up section from this lies the Marshall Paraconformity (Carter and Landis, 1972), a current-generated unconformity hypothesized to represent initiation of thermohaline circulation (Deep Western Boundary Current [DWBC]) and shallower circulation upon opening of the seaway between Antarctica and Australia, prior to the opening of the Drake Passage (Carter et al., 2004c). (Fulthorpe et al., 1996) dated the hiatus to signify a 3.4 m.y. (32.4-29 Ma) period of non-deposition or erosion using strontium isotopes. The Marshall Paraconformity occurs at the base of the Concord (mid-to-late Oligocene cross-bedded glauconitic sands) and Weka Pass (calcareous limestones) Formations that together comprise the Kekenodon Group (Carter, 1985, 1988).

Initiation of the first pulse of uplift and mountain building along the Alpine Fault was the result of increased convergence along the plate boundary and led to the deposition of regressive sediments within the basin. This regression spanned the Miocene to Recent and results from increased sediment supply from the uplifting of the Southern Alps. The Bluecliffs Formation is a widespread shelf siltstone dated as latest Oligocene or earliest Miocene. At some point in the mid to late Miocene (Tippett and Kamp, 1993a; Batt et al., 2000; Carter and Norris, 1976; Norris et al., 1978; Adams, 1979; Tippett and Kamp, 1993b) a second pulse of increased convergence along the Alpine fault led to an increase in fault transpression and subsequent increase in sediment supply (Lu et

al., 2005). This sediment influx was deposited within the basin as prograding clinoforms, forming the Otakou Group.

Northward flowing currents within the region have influenced deposition in the region since the latest Oligocene, with possible strengthening of these currents during glacial periods, and include such currents as the Southland (part of the Subtropical Front), and a local gyre of the Antarctic Circumpolar Current. Deposition of large sediment drifts within the prograding clinoforms, termed “Canterbury Drifts” by (Carter 2007), occurred under the influence of these currents (Fulthorpe and Carter, 1991; Lu et al., 2003; Carter et al., 2004c). Along with currents influencing deposition within the basin, basinal subsidence has also been present within the region and has been suggested to have begun ~8 Ma (Browne and Field, 1988) or possibly as early as 20 Ma. Increased convergence along the Alpine Fault may be the cause for increased basin subsidence (Lu et al., 2005).

IODP Leg 317

IODP Leg 317 set sail in late 2009 with the intention of exploring the offshore shallow continental margin within the Canterbury Basin, and in the process set several new scientific ocean drilling records (Expedition 317 Scientists, 2010). Included among these achievements are: (1) the second deepest hole in the history of scientific ocean drilling and deepest hole drilled during a single expedition (Hole U1352C, 1927 m); (2) the deepest hole drilled by the R/V *JOIDES Resolution* on a continental shelf (Hole U1351B, 1030 m); (3) the deepest microbiological sample ever taken for scientific ocean drilling (U1352, 1925 m); and (4) the shallowest depth for a site drilled by the R/V *JOIDES Resolution* (Expedition 317 Scientists, 2010). By delving into the thick sedimentary deposits of the continental shelf and slope,

scientists attempt to decipher how eustatic sea level change vs. local tectonic, sedimentary, and oceanographic processes govern continental margin depositional cyclicity.

The primary objective of Leg 317 was to date clinoform seismic sequence boundaries and sample associated facies to estimate eustatic amplitudes in order to further constrain sequence stratigraphic models with facies, paleoenvironments and depositional processes. Secondary objectives include: (1) An attempt to drill the Marshall Paraconformity in the hopes of providing information about its regional distribution, age, and origin (2) Constraining the erosional history of the Southern Alps by verifying the ages of prograding units within the basin and combining them with sedimentary volume data to develop a record of sedimentation rates for correlation with tectonic and climate events, and (3) Determination of sediment drift depositional history and paleoceanographic record.

Sediments recovered during this leg stretch from Eocene to Recent with a strong focus on the Miocene to Recent sediments, at which time global sea level was dominated by glacioeustacy. High rates of Neogene sediment supply resulted in the preservation of a high frequency (0.1-0.5 m.y.) depositional sediment cyclicity sourced by the erosional sediments of the nearby Southern Alps and shaped by strong offshore currents, which also contribute to the deposition of the many elongate sediment drifts present within the sediment prism. This IODP leg supplements past ocean drilling on the New Jersey margin (ODP Legs 150, 150X, 174A, 174AX and IODP Leg 313), in the Bahamas (ODP Leg 166), and other drilling within ENZOSS (ODP Leg 181). The sequence stratigraphic framework found within the New Jersey margin and Canterbury Basin are largely correlative, but Canterbury Basin sediments provide a record of the early development of the Antarctic circumpolar current and related oceanographic fronts in the area.(Expedition 317 Scientists, 2010)

Site U1352

The most basinward site of the Leg 317's Canterbury Basin drilling transect, Site U1352, is located on the upper slope of the Canterbury Bight ($44^{\circ} 56.2240'S$, $172^{\circ} 1.3615'E$). Four holes were drilled in 344 m of water that penetrated 14 sequence boundaries (U6-U19) (Fig. 3). Sediments here provide good age control for sequences drilled on the shelf due to a higher abundance of pelagic microfossils such as calcareous nannofossils and foraminifers.

The age of sediments from this site span the Holocene to late Eocene, reaching a depth of 1927 m, from which three distinctive lithologic units are described and further broken down into subunits (Expedition 317 Scientists, 2010). Unit 1 comprises the upper 711 m, spans the Holocene to middle Pliocene, and is subdivided into 3 subunits. Subunit 1A (0-98 m) consists of mostly clay with interbedded sand, clay and mud lithologies with frequent greenish-gray muddy sand or sandy mud beds with abrupt contacts. Subunit 1B (98-447 m) consists of mostly homogeneous muds and a reduction of the greenish gray muddy sand lithologies. Subunit 1C (447-711 m) consists of a transition from a clay-dominated unit to marl-dominated lithologies and incorporates some very fine sands with interbedded silt and mud. Unit 2 (711-1853 m), spanning the middle Pliocene to the early Eocene, continues this clay to marl transition, representing a gradual progression to deeper slope water depths. Unit 2 is divided into 3 subunits. Subunit 2A (711-1189 m) consists of a variation between homogeneous to bioturbated marl with interbedded silt and mud, and chalks. Subunit 2B (1189-1694 m) is composed of abundant dark-colored mud beds, marls and interbedded clay and mud. Subunit 2C (1694-1853 m) contains a transition from marls to chalk and limestone, with frequent glauconitic beds. Occurring at the base of Unit 2 is a ~12 m.y. unconformity showing an abrupt lithologic change into Unit 3 (1853-1927 m), that spans the early Oligocene to late Eocene. This unit contains chalk and limestone and lacks most siliciclastic constituents (Expedition 317 Scientists, 2010).

Hole U1352B

Hole U1352B, the primary object of study, was drilled to a depth of 830 mbsf, with a recovered interval of 613 m. Total recovery was 74%, with nearly 100% recovery throughout the Pleistocene (Fig. 4). Subunit 1A in this hole contains predominantly mud-rich sediment consisting of mud, interbedded mud-clay-sand, calcareous sandy mud, shelly muds, and muddy sands with common bioturbation. Subunit 1B consists of homogeneous mud intervals with greenish-gray marls that commonly contain carbonate cementation, interbedded sand and mud, mottled sandy mud and muddy sands with common bioturbation. Subunit 1C comprises a transition of mud-rich deposits to carbonate-rich sediments, but still contained mostly mud with marl, sandy mud and muddy sand. Hole U1352B drilled down through Subunit 2A as well, which consists mainly of homogeneous calcareous deposits but still contain a significant amount of detrital sand, silt and clay with cemented layers and concretions plus bioturbated marls that dominated the hole (Expedition 317 Scientists, 2010).

Objectives

Shipboard biostratigraphic interpretations tend to be rough estimations based on several factors, of which include the small amount of time analyzing each sample due fast-paced drilling operations and the type of sediment of which the samples are taken. During scientific drilling, sampling resolutions tend to be large due to the time required for a single sample analysis and the aforementioned pace of drilling. Many samples, as was the case for IODP Exp. 317, are taken from core catchers which sometimes yield sandy units yielding less-than-ideal assemblages. Due to these limitations of shipboard analysis, a more in depth shore-based biostratigraphic analysis is utilized to complement the shipboard biostratigraphic interpretation. Therefore, the chief objective of this project is to establish a finer resolution biostratigraphic framework that correlates with the on-ship analyses. Secondarily, an attempt will be made to constrain the age of

sequence stratigraphic boundaries observed through the Pleistocene section using calcareous nannofossil datums. Last, nannofossil abundance counts will be established with the aim of evaluating richness, evenness, and diversity within the Pleistocene section.

Continued research will be conducted on these samples in the future to examine abundance and age of reworked and transported nannofossil assemblages in a joint study with Stacie Blair, Laura Pea, and Cecilia McHugh. This study will analyze transport mechanisms and sediment sourcing in the Canterbury Basin region.

CHAPTER TWO

MATERIALS AND METHODS

Samples used in this study were recovered during Leg 317 of the Integrated Ocean Drilling Program (IODP) with an approximate sub-sampling resolution of four (4) meters. A simple smear-slide technique was utilized to prepare a small amount of sample for analysis. Slides were examined under an Axioscope II at 1250x magnification using a 100x oil immersion objective. Taxonomic classification for this study was based on (Bown, 1998; Perch-Nielsen, 1985; Bukry and Percival, 1971; de Kaenel et al, 1999; and Gartner, 1977). Nannofossil fragments of less than half a specimen were not included in the counts as to not count the same specimen twice. Counts were performed on up to 300 specimens to acquire semi-quantitative abundance data. At the end of each sample, one (1) extra traverse was performed in search of any rare taxa. Species' richness, evenness, and diversity were calculated using the "R" statistical analysis program and its "Vegan" package.

Calculation of Shannon diversity values followed the following formula:

$$H = - \sum_{i=1}^S p_i \log_b p_i$$

Where... p_i = proportion of species i

S = number of species so that $\sum_{i=1}^S p_i = 1$

b = base of the logarithm

Total nannofossil abundances were defined according to the following criteria:

V A (Very Abundant) = >90% of sediment particles

A (Abundant) = 50-90% of sediment particles

C (Common) = 15-50% of sediment particles

F (Few) = 1-15% of sediment particles

R (Rare) = <1% of sediment particles

Relative nannofossil abundances are recorded by the field of view (FOV) at 1250x

magnification:

D (Dominant) = >100 specimens/FOV

A (Abundant) = 10-100 specimens/FOV

C (Common) = 1-10 specimens/FOV

F (Few) = 1 specimen/1-10 FOVs

R (Rare) = 1 specimen/10-100 FOVs

P (Present) = 1 specimen/>100 FOVs

Nannofossil preservation was determined according to the following criteria:

G (Good) = Most specimens show little to no evidence of secondary alteration

(dissolution and/or recrystallization) and all specimens were identifiable to the species level.

M (Moderate) = Specimens show signs of dissolution and/or recrystallization, yet most specimens are still identifiable to the species level.

P (Poor) = Specimens show profound effects of secondary alteration and/or fragmentation. Most specimens are not identifiable to the species level but this is possible in some cases.

De Kaenel (1999)'s biostratigraphic datums and subsequent zonation scheme were used to further refine the shipboard biostratigraphy that followed (Martini, 1971) and (Gartner, 1977).

CHAPTER THREE

RESULTS

Abundance and Preservation

Preservation throughout the section fluctuates from poor to good, with areas of poorest preservation roughly correlating with observed sequence boundaries U14, U15, and U16. All sequence boundaries observed within the Pleistocene section at Site U1352 correlate with areas of moderate to poor preservation.

Calcareous nannofossils are common to abundant throughout the study interval (535.33 – 105.47 mbsf) with sporadic areas of few as well as very high abundance. Some of the areas of highest abundance strongly correlate with observed sequence boundaries U17 and U18, and roughly correlate with U16. Dominant background taxa throughout the section include *Calcidiscus leptoporus*, *Coccolithus pelagicus*, *Coccolithus pelagicus* aff. *braarudii*, *Cyclicargolithus floridanus*, *Gephyrocapsa aperta*, *Gephyrocapsa crassipons*, *Gephyrocapsa caribbeanica* (3-4 µm), *Helicosphaera carteri*, *Reticulofenestra haqii* (<3 µm), *Reticulofenestra haqii* (3-5 µm), *Reticulofenestra minuta*, and *Reticulofenestra minutula*. Additional background taxa present at lesser abundances include *Dictyococcites bisecta* and *Reticulofenestra dictyoda*. Some of these taxa, namely many of the reticulofenestrids, represent upper Miocene to Oligocene reworked assemblages although typical Pleistocene assemblages dominate the section and account for the majority of present taxa.

Species' Evenness, Richness and Diversity Indices

Species' richness, evenness and Shannon diversity were calculated for the Hole U1352B's Pleistocene nannofossil assemblage (Fig. 5). Species richness values range from 6 to 22 (excluding barren samples), averaging 13.99 species per sample. Samples corresponding with

noted sequence boundaries exhibit below average richness values (12.42). Species' evenness averages 0.51 and range from 0.11 to 0.79 (excluding barren samples). The average Shannon diversity value for this site is 1.35 with a range of 0.19 to 2.40.

An inverse pattern is noted between abundances of *Gephyrocapsa aperta* and Shannon diversity, evenness, and richness values (Fig. 5). *Gephyrocapsa aperta* abundances tend to be noticeably high in samples where its presence was recognized, leading to the conclusion that its abundance resulted in low evenness values throughout the Pleistocene section. Also, samples of low abundance of *G. aperta*, including samples where it does not occur, tend to have higher richness values than in samples where it is abundant. The dominance of *G. aperta* in most U1352B samples overshadowed abundances of most background taxa, explaining the relatively low diversity average.

Biostratigraphy

One hundred four samples were analyzed for this study. Twelve useful nannofossil datums were distinguished (Table 1; Fig. 6) following the de Kaenel (1999) zonation scheme, allowing 11 nannofossil zones/subzones or groups of zones to be used to biostratigraphically refine this Pleistocene section. Among these datums, seven FO (first occurrence) datums, four LO (last occurrence) datums and one FO acme were included. Of these twelve datums, six are based on size differentiations. Each datum and their corresponding biozones are discussed in more detail below:

Zone: 19A-7

Type of zone: Base zone

Definition: FO *Gephyrocapsa* sp. (>3 µm) to FO *Gephyrocapsa caribbeonica*

(>4µm)/*Gephyrocapsa oceanica* (>4 µm)

Age: 1.74 - 1.726 Ma

Duration: 0.11 million years

Remarks: Only the top portion of this zone/subzone was observed within the scope of this project and it is present in Sample U1352B-59X-2W, 60-61cm. This zone is based strictly by the absence of medium-sized Gephyrocapsids (>4 µm). This zone correlates to the uppermost portion of CN13A (Okada and Bukry, 1980), and falls in the middle of the *Calcidiscus macintyrei* Zone of (Gartner, 1977) and NN19A (Martini, 1971)

Zone: 19B-1 and 19C-1

Type of zone: Base Zone

Definition: FO *Gephyrocapsa caribbeonica* (>4 µm)/*Gephyrocapsa oceanica* (>4 µm) to FO *Gephyrocapsa oceanica* (>5.5 µm)

Age: 1.726 – 1.566 Ma

Duration: 0.160 million years

Remarks: The base of this zone was observed in sample U1352B-59X-2W, 60-61cm, while the top was marked at U1352B-51X-6W, 70-71cm. The presence of *Calcidiscus macintyrei* is quite obscure, and its final occurrence could not be accurately discerned. Therefore, the use of the LO of *Calcidiscus macintyrei* as a base for Zone 19C-1 was not applied to this study. Zones 19B-1 and 19C-1 correlate to the base of CN13B (Okada and Bukry, 1980).

Zone: 19D-1

Type of Zone: Base Zone

Definition: FO *Gephyrocapsa oceanica* ($>5.5\text{ }\mu\text{m}$) to FO *Gephyrocapsa oceanica* ($>6.5\text{ }\mu\text{m}$)

Age: 1.566 – 1.494 Ma

Duration: 0.072 million years

Remarks: Another useful datum found within this zone is the FO of *Gephyrocapsa caribbeanica* ($>6.5\text{ }\mu\text{m}$). Sample U1352B-46X-4W, 60-70 cm marks the top of the interval, and the base is within sample U1352B-51X-6W, 70-71cm. Zone 19D-1 falls within CN13B (Okada and Bukry, 1980), the *Helicosphaera sellii* Zone (Gartner, 1977), and NN19B (Martini, 1971).

Zone: 19E-1

Type of Zone: Base Zone

Definition: FO *Gephyrocapsa oceanica* ($>6.5\mu\text{m}$) to FO acme *Psuedoemiliania lacunosa*

Age: 1.494 – 1.361 Ma

Duration: 0.133 million years

Remarks: Sample U1352B-46X-4W, 60-70 cm marks the base of Zone 19E-1, with the top at Sample U1352B-46X-6W, 75-76 cm. Zone 19E-1 falls within CN13B (Okada and Bukry, 1980), *Helicosphaera sellii* Zone (Gartner, 1977), and NN19B (Martini, 1971).

Zones: 19F-1 and 19G-1

Type of Zone: Concurrent Range Zone

Definition: FO acme *Psuedoemiliania lacunosa* to LO *Gephyrocapsa sp.* ($>6.5\text{ }\mu\text{m}$)

Age: 1.361 – 1.235 Ma

Duration: 0.126 million years

Remarks: The acme of *P. lacunosa* is noted by an observed change from rare to few/common.

The base of Zone 19F-1 is found in sample U1352B-46X-6W, 75-76 cm, and the top of Zone 19G-1 was noted in Sample U1352B-43X-3W, 75-76 cm. The FO acme of *Gephyrocapsa aperta* could not be accurately determined due to its abundance throughout the section, therefore it was omitted as a datum for this study. Correlating with previous Pleistocene zonations, this zonal group correlates with the top of the *Helicosphaera sellii* Zone and base of the small *Gephyrocapsa* Zone of (Gartner, 1977), the top of CN13B (Okada and Bukry, 1980), and it comprises the bottom third of NN19B (Martini, 1971).

Zones: 19H-1, 19I-1, and 19I-2

Type of Zone: Partial Range Zone

Definition: LO *Gephyrocapsa* sp. (>6.5 µm) to FO *Gephyrocapsa omega*

Age: 1.235 – 0.962 Ma

Duration: 0.273 million years

Remarks: Sample U1352B-43X-3W, 75-76 cm marks the base of this zone, with the top found within Sample U1352B-32H-2W, 109-110 cm. The base and top of Zone 19I-1 are marked by the FO *Reticulofenestra asanoi* and the LcO (last common occurrence) *Reticulofenestra doronocoides*, respectively. *Reticulofenestra asanoi* is sparse within the samples and the species concept of *R. doronocoides* was not used in this study; therefore, these two datums could not be

identified. This zonal group can be correlated with nearly the entire small *Gephyrocapsa* Zone of (Gartner, 1977), it falls within the NN19B Zone of (Martini, 1971), and serves as the base of the CN14A Zone of (Okada and Bukry, 1980).

Zones: 19J-1, 19K-1, and 19K-2

Type of Zone: Concurrent Range Zone

Definition: FO *Gephyrocapsa omega* to LO *Reticulofenestra asanoi*

Age: 0.962 – 0.781 Ma

Duration: 0.181 million years

Remarks: This zone is marked by the FO of *G. omega* present in Sample U1352B-32H-2W, 109-110 cm and sample U1352B-29H-2W, 100-101 cm defines the top of the zonal group. *Reticulofenestra asanoi* was sparse and observed in only three samples, therefore, its last occurrence is tentatively placed at the top of this zonal group. This zonal group correlates with the base of the *Psuedoemiliania lacunosa* Zone of (Gartner, 1977), and falls within CN14A (Okada and Bukry, 1980) and NN19B (Martini, 1971).

Zones: 19L-1 and 19M-1

Type of Zone: Top Zone

Definition: LO *Reticulofenestra asanoi* to LO *Gephyrocapsa omega*

Age: 0.781 – 0.584 Ma

Duration: 0.197 million years

Remarks: LO *R. asanoi* defines the base of this zonal group and occurs in Sample U1352B-29H-2W, 100-101 cm. Sample U1352B-27H-6W, 55-56 cm marks the top of this biozone.

Separation of Zones 19L-1 and 19M-1 could not be discerned due to the lack of the LO acme of *Psuedoemiliania lacunosa ovata*. These two zones occur within CN14A (Okada and Bukry, 1980), NN19B (Martini, 1971), and the *Psuedoemiliania lacunosa* zone (Gartner, 1977).

Zones: 19M-2, 19N-1 and 19O-1

Type of Zone: Top Zone

Definition: LO *Gephyrocapsa omega* to LO *Psuedoemiliania lacunosa* sp.

Age: 0.584 – 0.406 Ma

Duration: 0.178 million years

Remarks: Sample U1352B-27H-6W, 55-56 cm and sample U1352B 26H-4W, 75-76 cm are documented as the base and top of this biozone group, respectively. Marking the base of Zone 19N-1 is the FO acme of *G. caribbeonica*, but this was not observed within the section; therefore, it is not used to further subdivide this zonal group. A strong correlation exists between these two zones and the tops of CN14A (Okada and Bukry, 1980), NN19B (Martini, 1971), and the LO of *Psuedoemiliania lacunosa*.

Zone: 20A-1

Type of Zone: Top Zone

Definition: LO *Psuedoemiliania lacunosa* sp. to LO acme *Gephyrocapsa caribbeonica*

Age: 0.406 – 0.262 Ma

Duration: 0.144 million years

Remarks: The base of this zone was noted in Sample U1352B-26H-4W, 75-76 cm. A valuable datum occurring near the top of the zone is the FO of *Emiliania huxleyi*, which is noted in Sample U1352B-12H-6W, 80-81 cm. Abundances of *Gephyrocapsa caribbeonica* (3-4 µm) do not seem to fluctuate towards the uppermost samples analyzed, thereby leading to the conclusion that Zone NN21B-1 was not reached in the scope of this study. Zone 20A-1 is the (de Kaenel, 1999) equivalent of Martini's (1971) NN20, Okada and Bukry's (1980) CN14B, and the *Gephyrocapsa oceanica* Zone of (Gartner, 1977).

CHAPTER FOUR

DISCUSSION

Calcareous Nannofossil Datums

De Kaenel (1999) established twenty calcareous nannofossil datums throughout the Pleistocene, of which twelve were delineated and used to decipher ages for the U1352 Pleistocene section (Table 1; Fig 6). Datum 1 (FO *Emiliania huxleyi* > *Gephyrocapsa spp.*) and Datum 2 (FcO *Emiliania huxleyi*) were not reached and seven other datums (5, 6, 9, 11, 11b, 16 and 17) could not be identified within the given samples. Datum 17, the LO *Calcidiscus macintyrei* (>11 μ m), could not be established within the section due to low abundances and sporadic occurrences. Datum 16 is given as the FO *Gephyrocapsa* sp. (>5 μ m), and while specimens of *Gephyrocapsa* were found within this range, the species concept for this project differentiates the gephyrocapsids into the following size determinations: *G. aperta/crassipons* <3 μ m), *G. caribbeanica/oceanica* (3-4.5 μ m), *G. caribbeanica/oceanica* (4.5-5.5 μ m), *G. caribbeanica/oceanica* (>5.5 μ m), and *G. caribbeanica/oceanica* (>6.5 μ m). Attention was not paid to distinguishing gephyrocapsids using a 5 μ m-size criterion, and Datum 16 could not be identified.

The LcO of *Helicosphaera sellii* serves as Datum 11, but was not observed within U1352B sediments. The abundance of *H. sellii* becomes sparse toward the upper extent of its range, with values of few to rare. The LO of *H. sellii* (Datum 11b) is also difficult to discern because of the species' low abundances. Sample U1352B-44X-4W, 75-76 cm represents the last *H. sellii* observed, but cannot be confidently used to represent its true last occurrence. The zonation scheme employed here distinguishes the LO of *H. sellii* as a secondary marker, thereby providing an adequate zonation without taking it into account.

Datum 9, according to de Kaenel (1999), is defined as the FO of *Reticulofenestra asanoi*. This species occurred within only three samples, and its abundance in each sample is few to rare. This provides no distinct way to ascertain its first occurrence, and this datum could not be distinguished. The LO acme of *Psuedoemiliania lacunosa ovata* provides the marker for Datum 6, but it could not be documented here. *Psuedoemiliania ovata*, throughout this Pleistocene section, was encountered in only three samples with an abundance of common or higher. This species was present with abundances of 1 specimen per 1-10 fields of view (few). As an acme is based on major fluctuations in a given species' abundance, of which no such fluctuations were present for *P. ovata*, Datum 6 was not used in this study. Additionally, the LO of *Psuedoemiliania lacunosa lacunosa* (Datum 5) occurred simultaneously in our sequence with the LO of *Psuedoemiliania lacunosa* sp.(Datum 4), and was therefore, omitted here. Instead, Datum 4 is used and represents the last occurrence of the *Psuedoemiliania lacunosa* lineage.

A datum not proposed in de Kaenel (1999), but found to work particularly well as a zonal marker here is the LO of *Gephyrocapsa omega*. This marker is described as the base of Zone 19M-2 and is distinguished by its immediate and abrupt reduction in abundance from common to barren. This last occurrence provides an additional datum to refine our Pleistocene biostratigraphy.

Sequence Boundaries

Shipboard nannofossil dating provided robust age control throughout the Pleistocene section (Expedition 317 Scientists, 2010) and is used to date the seismically mapped sequence boundaries. Of the seven observed sequence boundaries (U13-U19) in the Pleistocene section at Site U1352, six (U13-U18) are found within the interval examined in this study. Constrained age ranges of these boundaries derived aboard ship and in this study are provided in (Table 2). This

study found that around these sequence boundaries, calcareous nannofossil abundance values were above average (common to abundant). For a few of these boundaries (U14, U15, and U16), however, below average abundances (few to common) were documented directly below the boundary. Reasons for these sparse patterns within the data are as of yet unknown.

Richness and preservation values of the samples representing the predicted sequence boundaries were below average (12.43 and 4.21, respectively). Reduced preservation within these intervals can be explained through an increase of porosity in these sandy-marl lithologies. Dissolution and reprecipitation of calcareous material takes place within such porous materials, resulting in overall moderate to poor preservation.

CHAPTER FIVE

SUMMARY AND CONCLUSIONS

Twelve biostratigraphic datums along with ten biozones/zonal groups were recognized in the semi-quantitative abundance data from Hole U1352B using de Kaenel's 1999 zonation scheme. Several datums, including the traditionally utilized LO of *H. sellii*, LO of *Calcidiscus macintyreai*, and FO/LO of *Gephyrocapsa* spp. small (*G. aperta*), remained indistinguishable or unclear in the data. Shifts in preservation/abundance correlate, at some points, with the predicted depths of sequence boundaries. Values of diversity, evenness, and richness show robust inverse correlations with abundance of *Gephyrocapsa aperta* throughout the entire Pleistocene in the Canterbury Basin.

Publication of these semi-quantitative nannofossil data as a data report will take place within the IODP Leg 317 Scientific Volume. Also, data and findings from this project will be compared with data from 3 additional sites (U1351, U1353, and U1354) to derive a more comprehensive understanding of nannofossil assemblages, reworking, and sediment transport in the Canterbury Basin region.

APPENDIX A

TAXONOMIC LIST

- Braarudosphaera bigelowii* Gran and Braarud, 1935
- Calcidiscus leptoporus* Murray and Blackman, 1898
- Calcidiscus macintyreai* Bukry and Bramlette, 1969b
- Coccolithus pelagicus* Wallich, 1877
- Coccolithus pelagicus* f. *braarudii* (Gaarder) Geisen *et al.* 2002
- Coccolithus streckeri* Takayama and Sato, 1986
- Cyclicargolithus abisectus* Müller, 1970
- Cyclicargolithus floridanus* Roth and Hay in Hay *et al.*, 1967
- Dictyococcites bisectus* <10 µm Hay, Mohler and Wade, 1966
- Dictyococcites bisectus* Hay, Mohler and Wade, 1966
- Dictyococcites productellus* (3-5 µm) Kamptner, 1963
- Dictyococcites scrippsae* Bukry and Percival, 1971
- Discoaster deflandrei* Bramlette and Riedel, 1954
- Emiliania huxleyi* Lohmann, 1902
- Gephyrocapsa aperta* Kamptner, 1963
- Gephyrocapsa crassipons* Okada and McIntyre, 1977
- Gephyrocapsa caribbeanica* (3-4 µm) Boudreux and Hay, 1967
- Gephyrocapsa caribbeanica* (4-5.5 µm) Boudreux and Hay, 1967
- Gephyrocapsa caribbeanica* (>5.5µm) Boudreux and Hay, 1967
- Gephyrocapsa caribbeanica* (>6.5 µm) Boudreux and Hay, 1967
- Gephyrocapsa oceanica* (3-4 µm) Kamptner, 1943
- Gephyrocapsa oceanica* (4-5.5 µm) Kamptner, 1943
- Gephyrocapsa oceanica* (>5.5 µm) Kamptner, 1943
- Gephyrocapsa oceanica* (>6.5 µm) Kamptner, 1943
- Gephyrocapsa omega* Bukry, 1973c
- Helicosphaera carteri* Wallich, 1877
- Helicosphaera* cf. *sellii* Bukry and Bramlette, 1969b
- Helicosphaera sellii* Bukry and Bramlette, 1969b

- Pontosphaera discopora* Schiller, 1925
Pontosphaera japonica Takayama, 1967
Pontosphaera multipora Kamptner, 1948
Psuedoemiliania lacunosa Kamptner, 1963
Psuedoemiliania ovata Bukry, 1973
Psuedoemiliania pacifica Young, 1990
Reticulofenestra amplus Gartner, 1992
Reticulofenestra asanoi Sato and Takayama, 1992
Reticulofenestra daviesi Haq, 1968
Reticulofenestra dictyoda Deflandre in Deflandre and Fert, 1954
Reticulofenestra filewiczii Wise and Weigand in Wise, 1983
Reticulofenestra gelida Geitzenauer, 1972
Reticulofenestra haqii (<3 µm) Backman, 1978
Reticulofenestra haqii (3-5 µm) Backman, 1978
Reticulofenestra minuta Roth, 1970
Reticulofenestra minutula Gartner, 1967
Reticulofenestra psuedoumbilica Gartner, 1967
Thoracosphaera sp.

APPENDIX B

TABLES

Table 1: Calcareous nannofossil datums and ages in Hole U1352B

Datum No. (de Kaenel, 1999)	Event	Datum	Age (Ma)	Depth (mbsf)	Core, Section, Interval
3	FO	<i>Emiliania huxleyi</i>	0.270	111.47	12H-6W, 80-81cm
4	LO	<i>Psuedoemiliania lacunosa</i>	0.406	232.38	26H-4W, 75-76cm
-	LO	<i>Gephyrocapsa omega</i>	0.584	244.46	27H-4W, 55-56cm
7	LO	<i>Reticulofenestra asanoi</i>	0.781	253.71	29H-2W, 100-101cm
8	FO	<i>Gephyrocapsa omega</i>	0.962	274.81	32H-2W, 109-110cm
10	LO	<i>Gephyrocapsa sp.</i> (>6.5 µm)	1.235	354.46	43X-2W, 75-76cm
12	FO acme	<i>Psuedoemiliania lacunosa</i>	1.361	368.66	44X-6W, 75-76cm
13	FO	<i>Gephyrocapsa oceanica</i> (>6.5 µm)	1.494	384.78	46X-4W, 69-70cm
14	FO	<i>Gephyrocapsa caribbeanica</i> (>6.5 µm)	1.525	412.06	49X-3W, 75-76cm
15	FO	<i>Gephyrocapsa oceanica</i> (>5.5 µm)	1.566	436.91	51X-6W, 70-71cm
18	FO	<i>Gephyrocapsa oceanica</i> (>4 µm)	1.719	480.75	56X-4W, 74-75cm
18b	FO	<i>Gephyrocapsa caribbeanica</i> (>4 µm)	1.726	506.41	59X-2W, 60-61cm

Table 2: Age constraints of observed sequence boundaries in Hole U1352B derived from calcareous nannofossil age datums.

Sequence Boundary	Datum	Age (Ma) – THIS STUDY	Age Constraint – Shipboard Biostratigraphy
U13	FO <i>G. oceanica</i> (>4 µm) – FO <i>G. oceanica</i> (>5.5 µm)	1.726–1.566	1.81–1.69
U14	FO <i>G. oceanica</i> (>4 µm) – FO <i>G. oceanica</i> (>5.5 µm)	1.726–1.566	1.69–1.56
U15	FO <i>G. oceanica</i> (>5.5 µm) – FO <i>G. oceanica</i> (>6.5 µm)	1.566–1.525	1.69–1.56
U16	LO <i>R. asanoi</i> – LO <i>G. omega</i>	0.781–0.584	0.91–0.44
U17	LO <i>P. lacunosa</i> – FO <i>E. huxleyi</i>	0.406–0.270	0.91–0.44
U18	LO <i>P. lacunosa</i> – FO <i>E. huxleyi</i>	0.406–0.270	0.44–0.29

Table 3: Pleistocene relative calcareous nannofossil abundance from Hole U1352B.

Core	Section	Sample Interval	Core Top Depth (mbsf)	Sample	Top Depth (mbsf)	CSF-A	Nanno Abundance	Bottom Depth (mbsf)	Abund (Numerical)	Preservation	Pres (Numerical)	Total Abundance	Diversity	<i>Braarudosphaera bigelowi</i>	<i>Calcidiscus leptoporus</i>	<i>Calcidiscus macintyrei</i>	<i>Coccolithus pelagicus</i>	<i>Coccolithus pelagicus f. braarud</i>	<i>Coccolithus streckeri</i>	<i>Cyclaragonolithus abisectus</i>	<i>Cyclaragonolithus floridanus</i>	<i>Cyclagelosphaera</i> sp.	<i>Dictyococcites bisectus</i>	<i>Dictyococcites productilis</i> /3-5	<i>Dictyococcites scriptae</i>	<i>Discoaster deflandrei</i>
12	2	76-77	104.7	105.46	105.47		C	3.0	M	4	303	19			3		20	4	1				P			
12	6	80-81	110.66	111.46	111.47	A	4.0	G	5	309	14			P		15	1						P			
13	5	69-70	118.68	119.37	119.38	A-C	3.5	G	5	304	11			1		22	1									
14	1	70-71	122.2	122.9	122.91	A-C	3.5	G	5	309	15			2		11	3	2					1	1		
14	5	130-131	128.2	129.5	129.51	A	4.0	G	5	306	18			P		18	5						1	1		
15	4	51-52	136.13	136.64	136.65	A	4.0	G	5	303	15															
16	2	74-75	142.7	143.44	143.45	A	4.0	G	5	305	16					18	17	2					9			
16	6	79-80	148.67	149.46	149.47	VA	5.0	G	5	332	8					19	11	2								
17	4	54-55	154.49	155.03	155.04	A	4.0	G	5	316	12			P		3	1	1	1							
18	4	25-26	160.27	160.52	160.53	A	4.0	G	5	309	17			2		9	7	P	P	1			P			
19	2	70-71	167.2	167.9	167.91	F	2.0	M	4	100	11					41	10							1		
19	6	27-28	173.17	173.44	173.45	B	0.0	-	0	0	0															
21	2	72-73	181.2	181.92	181.93	A	4.0	G	5	319	9			1				10								
22	2	74-75	190.7	191.44	191.45	A	4.0	G	5	340	12			P				17		P	P					
22	5	75-76	195.2	195.95	195.96	VA	5.0	G-M	4.5	347	6			2				15								
23	2	74-75	200.2	200.94	200.95	C	3.0	G	5	302	8							24		P		1				
23	4	75-76	203.2	203.95	203.96	C	3.0	M	4	302	10					27	23		4					P		
23	6	100-101	206.2	207.2	207.21	A-C	3.5	G	5	311	13			1		22	11		2		P					
24	5	63-64	214.2	214.83	214.84	A	4.0	G	5	304	11					8	15		1		1	1		P		
25	3	75-76	220.7	221.45	221.46	C	3.0	G	5	308	13					1	1		P							
25	7	40-41	226.2	226.6	226.61	A	4.0	M	4	303	12					2	1						8			
26	4	75-76	231.62	232.37	232.38	VA	5.0	G	5	303	8					4	1									
27	2	25-26	238.2	238.45	238.46	VA	5.0	G	5	302	6					4		1								
27	4	55-56	241.2	241.75	241.76	VA	5.0	G	5	322	4			1		9										
27	6	25-26	244.2	244.45	244.46	VA	5.0	G	5	317	9					8	2									
28	2	112-113	247.63	248.75	248.76	A	4.0	G	5	304	12			6		7			2							
28	3	83-84	249.13	249.96	249.97	A	4.0	M	4	302	18			18	1	25	5		2							
28	4	47-48	250.13	250.6	250.61	C	3.0	M-P	3.5	302	22			3		32	1		17		2		1			
29	2	100-101	252.7	253.7	253.71	F	2.0	M	4	303	18			3		19		1	40	1	1	1	1			
30	2	89-90	259.2	260.09	260.1	F	2.0	G-M	4.5	303	17			1		21	1							1		
30	4	89-90	262.2	263.09	263.1	F	2.0	G-M	4.5	301	22	1	2			52	3	1	40		2					
31	5	113-114	271.01	272.14	272.15	C	3.0	G	5	314	19			1		25	3		6					1		
32	2	109-110	273.7	274.8	274.81	C	3.0	G-M	4.5	319	8					16	3		1							
32	4	110-111	276.7	277.79	277.8	A	4.0	M	4	301	11					4			4							
33	2	33-34	283.11	283.44	283.45	C	3.0	M	4	301	6			3		66	3									
33	4	89-90	284.64	285.53	285.54	A	4.0	G	5	303	13			1		7	2		3		1					
33	6	23-24	287.62	287.85	287.86	A-C	3.5	M	4	301	7					16	5	1	4							
34	2	100-101	288.46	289.46	289.47	A	4.0	G-M	4.5	301	12								P		P					
34	4	14-15	290.77	290.91	290.92	A	4.0	G-M	4.5	304	8					6	1		5							
35	2	46-47	294.34	294.8	294.81	A	4.0	G	5	309	11			2		11	4		1							
36	2	14-15	296.5	296.64	296.65	F	2.0	M	4	305	10					4	1		2					1		
38	2	75-76	304.1	304.85	304.86	C	3.0	M	4	302	12					7		13								
38	6	35-36	310.1	310.45	310.46	F	2.0	G	5	301	13					2		11	2							
39	4	79-80	316.7	317.49	317.5	F	2.0	M	4	301	14	1	15			30	1		3							
40	1	105-106	321.9	322.95	322.96	F	2.0	G	5	304	13			1		4			1	1						
40	2	75-76	323.4	324.15	324.16	C	3.0	G-M	4.5	304	7					4		25	2							
40	3	105-106	324.9	325.95	325.96	A	4.0	M	4	319	14			8		37	1		2							
40	4	75-76	326.4	327.15	327.16	C	3.0	M	4	303	15					3			2		P					
41	2	75-76	333	333.75	333.76	C	3.0	M	4	300	13			22		52	8		3							
41	4	61-62	336	336.61	336.62	C	3.0	G-M	4.5	303	20	P	8			85	13	1	2	3	4		1			
41	6	69-70	339	339.69	339.7	F-C	2.5	G	5	311	17			2		90	29		5							
42	1	80-81	341.1	341.9	341.91	F	2.0	P	3	302	17			2		9	1		P		1					
42	3	80-81	344.1	344.9	344.91	F	2.0	G	5	301	20			4		2			1		15					
42	4	79-80	345.6	346.39	346.4	F	2.0	G	5	306	18			11		3	1		1							
43	2	75-76	352.2	352.95	352.96	F	2.0	G-M	4.5	304	18			5		14	5		6	4	2	2				
43	3	75-76	353.7	354.45	354.46	C	3.0	G	5	300	16			2		4	1		2	1	7					
43	5	75-76	356.7	357.45	357.46	A	4.0	G	5	303	25	1	3			4										
43	7	45-46	359.2	359.65	359.66	A	4.0	G	5	304	17			6		6	1		2							

Table 3 - continued

Core Section	Sample Interval	Core Top Depth (mbsf)		Sample Top Depth (mbsf) CSF-A		Sample Bottom Depth (mbsf) CSF-A		Total Abundance	Diversity		
		Core Top Depth (mbsf)	Sample Top Depth (mbsf)	Core Top Depth (mbsf)	Sample Top Depth (mbsf)	Core Top Depth (mbsf)	Sample Top Depth (mbsf)			Core Top Depth (mbsf)	Sample Top Depth (mbsf)
12	2	76-77	104.7	105.46	105.47	303	19	A	F	F	
12	6	80-81	110.66	111.46	111.47	309	14	A		C	
13	5	69-70	118.68	119.37	119.38	304	11	C		F	
14	1	70-71	122.2	122.9	122.91	309	15	C		C	
14	5	130-131	128.2	129.5	129.51	306	18	C	F	C	
15	4	51-52	136.13	136.64	136.65	303	15	F	R	F	
16	2	74-75	142.7	143.44	143.45	305	16	C	F	C	
16	6	79-80	148.67	149.46	149.47	332	8			C	
17	4	54-55	154.49	155.03	155.04	316	12			F	
18	4	25-26	160.27	160.52	160.53	309	17	C		C	F
19	2	70-71	167.2	167.9	167.91	100	11	F			
19	6	27-28	173.17	173.44	173.45	0	0				
21	2	72-73	181.2	181.92	181.93	319	9	A	C	F	
22	2	74-75	190.7	191.44	191.45	340	12	A		C	
22	5	75-76	195.2	195.95	195.96	347	6	D		F	
23	2	74-75	200.2	200.94	200.95	302	8		C		
23	4	75-76	203.2	203.95	203.96	302	10	R	C	R	
23	6	100-101	206.2	207.2	207.21	311	13	C	C		
24	5	63-64	214.2	214.83	214.84	304	11	C	A	R	
25	3	75-76	220.7	221.45	221.46	308	13	C	A	F	
25	7	40-41	226.2	226.6	226.61	303	12	C	A	C	
26	4	75-76	231.62	232.37	232.38	303	8	D			
27	2	25-26	238.2	238.45	238.46	302	6	A	C		P
27	4	55-56	241.2	241.75	241.76	322	4	D			
27	6	25-26	244.2	244.45	244.46	317	9	D	C		
28	2	112-113	247.63	248.75	248.76	304	12	A		F	
28	3	83-84	249.13	249.96	249.97	302	18	A	F	F	R
28	4	47-48	250.13	250.6	250.61	302	22	C	R	F	
29	2	100-101	252.7	253.7	253.71	303	18	C	R	F	
30	2	89-90	259.2	260.09	260.1	303	17	C	F	F	
30	4	89-90	262.2	263.09	263.1	301	22	C	F	F	
31	5	113-114	271.01	272.14	272.15	314	19	A	F	R	
32	2	109-110	273.7	274.8	274.81	319	8	A			
32	4	110-111	276.7	277.79	277.8	301	11	C	F	R	
33	2	33-34	283.11	283.44	283.45	301	6	A			
33	4	89-90	284.64	285.53	285.54	303	13	A	F		
33	6	23-24	287.62	287.85	287.86	301	7	A			
34	2	100-101	288.46	289.46	289.47	301	12	A			
34	4	14-15	290.77	290.91	290.92	304	8	A			
35	2	46-47	294.34	294.8	294.81	309	11	A	F		
36	2	14-15	296.5	296.64	296.65	305	10	A		R	P
38	2	75-76	304.1	304.85	304.86	302	12	A	F	F	
38	6	35-36	310.1	310.45	310.46	301	13	A	F	R	
39	4	79-80	316.7	317.49	317.5	301	14	C	R	R	
40	1	105-106	321.9	322.95	322.96	304	13	C	F	R	
40	2	75-76	323.4	324.15	324.16	304	7	A			
40	3	105-106	324.9	325.95	325.96	319	14	A	F	C	
40	4	75-76	326.4	327.15	327.16	303	15	C		F	
41	2	75-76	333	333.75	333.76	300	13	C	C		
41	4	61-62	336	336.61	336.62	303	20	C	F	R	
41	6	69-70	339	339.69	339.7	311	17	C	C	F	
42	1	80-81	341.1	341.9	341.91	302	17	C	C	R	
42	3	80-81	344.1	344.9	344.91	301	20	C	C	F	
42	4	79-80	345.6	346.39	346.4	306	18	C	C	F	
43	2	75-76	352.2	352.95	352.96	304	18	C	F	R	
43	3	75-76	353.7	354.45	354.46	300	16	C	F	F	
43	5	75-76	356.7	357.45	357.46	303	25	C	C	F	
43	7	45-46	359.2	359.65	359.66	304	17	C	C	C	

Table 3 - continued

Core Section	Sample Interval	Core Top Depth (mbsf)	Sample Top Depth (mbsf) CSF-A	Sample Bottom Depth (mbsf) CSF-A	Total Abundance	Diversity	<i>Pontosphaera discopora</i>	<i>Pontosphaera japonica</i>	<i>Pontosphaera multipora</i>	<i>Pseudoeumiliaria lacunosa</i>	<i>Pseudoeumiliaria ovata</i>	<i>Reticulofenestra amplis</i>	<i>Reticulofenestra asanoi</i>	<i>Reticulofenestra daviesi</i>	<i>Reticulofenestra dictyoda</i>	<i>Reticulofenestra filewiczi</i>	<i>Reticulofenestra gelida</i>	<i>Reticulofenestra haqii (<3)</i>	<i>Reticulofenestra haqii (3-5)</i>
12	2	76-77	104.7	105.46	105.47	303	19											R	
12	6	80-81	110.66	111.46	111.47	309	14										P	F	
13	5	69-70	118.68	119.37	119.38	304	11												
14	1	70-71	122.2	122.9	122.91	309	15												
14	5	130-131	128.2	129.5	129.51	306	18										P	C	F
15	4	51-52	136.13	136.64	136.65	303	15										P	F	
16	2	74-75	142.7	143.44	143.45	305	16										P	F	F
16	6	79-80	148.67	149.46	149.47	332	8										F	C	
17	4	54-55	154.49	155.03	155.04	316	12												
18	4	25-26	160.27	160.52	160.53	309	17										R	R	F
19	2	70-71	167.2	167.9	167.91	100	11												
19	6	27-28	173.17	173.44	173.45	0	0												
21	2	72-73	181.2	181.92	181.93	319	9												
22	2	74-75	190.7	191.44	191.45	340	12												
22	5	75-76	195.2	195.95	195.96	347	6												
23	2	74-75	200.2	200.94	200.95	302	8												
23	4	75-76	203.2	203.95	203.96	302	10												
23	6	100-101	206.2	207.2	207.21	311	13										R	P	F
24	5	63-64	214.2	214.83	214.84	304	11										R	R	
25	3	75-76	220.7	221.45	221.46	308	13												
25	7	40-41	226.2	226.6	226.61	303	12												
26	4	75-76	231.62	232.37	232.38	303	8										F	F	R
27	2	25-26	238.2	238.45	238.46	302	6												F
27	4	55-56	241.2	241.75	241.76	322	4												
27	6	25-26	244.2	244.45	244.46	317	9										P		
28	2	112-113	247.63	248.75	248.76	304	12	P									P	F	F
28	3	83-84	249.13	249.96	249.97	302	18	F										F	F
28	4	47-48	250.13	250.6	250.61	302	22											F	F
29	2	100-101	252.7	253.7	253.71	303	18	R									P	R	
30	2	89-90	259.2	260.09	260.1	303	17										R	F	R
30	4	89-90	262.2	263.09	263.1	301	22										R	R	
31	5	113-114	271.01	272.14	272.15	314	19										R	F	F
32	2	109-110	273.7	274.8	274.81	319	8	F									F		
32	4	110-111	276.7	277.79	277.8	301	11										R	R	R
33	2	33-34	283.11	283.44	283.45	301	6		P								F		P
33	4	89-90	284.64	285.53	285.54	303	13	P									F	F	
33	6	23-24	287.62	287.85	287.86	301	7										P	P	
34	2	100-101	288.46	289.46	289.47	301	12										F		
34	4	14-15	290.77	290.91	290.92	304	8										P	F	
35	2	46-47	294.34	294.8	294.81	309	11	P									P	R	F
36	2	14-15	296.5	296.64	296.65	305	10	R											C
38	2	75-76	304.1	304.85	304.86	302	12												R
38	6	35-36	310.1	310.45	310.46	301	13		F									F	F
39	4	79-80	316.7	317.49	317.5	301	14	R										R	F
40	1	105-106	321.9	322.95	322.96	304	13											R	F
40	2	75-76	323.4	324.15	324.16	304	7												
40	3	105-106	324.9	325.95	325.96	319	14										F	P	C
40	4	75-76	326.4	327.15	327.16	303	15		P								F	F	R
41	2	75-76	333	333.75	333.76	300	13	F									F		F
41	4	61-62	336	336.61	336.62	303	20	R	R								P	R	F
41	6	69-70	339	339.69	339.7	311	17	F										F	F
42	1	80-81	341.1	341.9	341.91	302	17	F					R	R			R	R	R
42	3	80-81	344.1	344.9	344.91	301	20	F	R				F	R			F	F	
42	4	79-80	345.6	346.39	346.4	306	18	R					F	F			C		
43	2	75-76	352.2	352.95	352.96	304	18										R	R	R
43	3	75-76	353.7	354.45	354.46	300	16	P	P	P	F						R	F	
43	5	75-76	356.7	357.45	357.46	303	25	R			R	C				F	P	F	C
43	7	45-46	359.2	359.65	359.66	304	17	P			F	F				F		R	C

Table 3 - continued

Core Section	Sample Interval	Core Top Depth (mbsf)	Sample Top Depth (mbsf) CSF-A	Sample Bottom Depth (mbsf) CSF-A	Total Abundance	Diversity	Fields Of View		
							Reticulofenestra minuta	Reticulofenestra minutula	Reticulofenestra pseudounbilica
12 2	76-77	104.7	105.46	105.47	303	19	C	F	P
12 6	80-81	110.66	111.46	111.47	309	14	C	C	
13 5	69-70	118.68	119.37	119.38	304	11	C		
14 1	70-71	122.2	122.9	122.91	309	15	C	F	
14 5	130-131	128.2	129.5	129.51	306	18	F	F	
15 4	51-52	136.13	136.64	136.65	303	15	C	F	
16 2	74-75	142.7	143.44	143.45	305	16	C	C	
16 6	79-80	148.67	149.46	149.47	332	8	F		
17 4	54-55	154.49	155.03	155.04	316	12	C	F	
18 4	25-26	160.27	160.52	160.53	309	17	F	F	
19 2	70-71	167.2	167.9	167.91	100	11	R	R	100
19 6	27-28	173.17	173.44	173.45	0	0			
21 2	72-73	181.2	181.92	181.93	319	9	A	F	
22 2	74-75	190.7	191.44	191.45	340	12	A	F	
22 5	75-76	195.2	195.95	195.96	347	6	C		
23 2	74-75	200.2	200.94	200.95	302	8	F		
23 4	75-76	203.2	203.95	203.96	302	10			P
23 6	100-101	206.2	207.2	207.21	311	13			
24 5	63-64	214.2	214.83	214.84	304	11	F		
25 3	75-76	220.7	221.45	221.46	308	13	F	F	P
25 7	40-41	226.2	226.6	226.61	303	12	R		
26 4	75-76	231.62	232.37	232.38	303	8	F		P
27 2	25-26	238.2	238.45	238.46	302	6			
27 4	55-56	241.2	241.75	241.76	322	4			
27 6	25-26	244.2	244.45	244.46	317	9	C		
28 2	112-113	247.63	248.75	248.76	304	12		F	
28 3	83-84	249.13	249.96	249.97	302	18	F		
28 4	47-48	250.13	250.6	250.61	302	22	F	R	R
29 2	100-101	252.7	253.7	253.71	303	18	F		
30 2	89-90	259.2	260.09	260.1	303	17	F		
30 4	89-90	262.2	263.09	263.1	301	22	R		R
31 5	113-114	271.01	272.14	272.15	314	19	F	R	R
32 2	109-110	273.7	274.8	274.81	319	8	F		
32 4	110-111	276.7	277.79	277.8	301	11	F		
33 2	33-34	283.11	283.44	283.45	301	6			
33 4	89-90	284.64	285.53	285.54	303	13	F		F
33 6	23-24	287.62	287.85	287.86	301	7	F		P
34 2	100-101	288.46	289.46	289.47	301	12	F	F	
34 4	14-15	290.77	290.91	290.92	304	8			
35 2	46-47	294.34	294.8	294.81	309	11			
36 2	14-15	296.5	296.64	296.65	305	10		P	
38 2	75-76	304.1	304.85	304.86	302	12		F	
38 6	35-36	310.1	310.45	310.46	301	13	R		
39 4	79-80	316.7	317.49	317.5	301	14		R	
40 1	105-106	321.9	322.95	322.96	304	13	R		
40 2	75-76	323.4	324.15	324.16	304	7			
40 3	105-106	324.9	325.95	325.96	319	14		R	
40 4	75-76	326.4	327.15	327.16	303	15	F	R	
41 2	75-76	333	333.75	333.76	300	13	R		
41 4	61-62	336	336.61	336.62	303	20	R	R	
41 6	69-70	339	339.69	339.7	311	17	R	R	
42 1	80-81	341.1	341.9	341.91	302	17	R		
42 3	80-81	344.1	344.9	344.91	301	20	R	R	
42 4	79-80	345.6	346.39	346.4	306	18	R	F	
43 2	75-76	352.2	352.95	352.96	304	18			R
43 3	75-76	353.7	354.45	354.46	300	16		R	
43 5	75-76	356.7	357.45	357.46	303	25	R	F	
43 7	45-46	359.2	359.65	359.66	304	17	F		

Table 3 - continued

Core Section	Sample Interval	Core Top Depth (mbsf)			Sample Top Depth (mbsf) CSF-A			Sample Bottom Depth (mbsf) CSF-A			Total Abundance	Diversity
		44	2	85-86	361.9	362.75	362.76	300	19	R	<i>Braarudosphaera bigelowi</i>	
44	4	75-76	364.9	365.65	365.66	305	16	F	F	F	<i>Calcidiscus leptоторus</i>	
44	6	75-76	367.9	368.65	368.66	301	20	F	F	F	<i>Calcidiscus macintyrei</i>	
45	2	76-77	371.5	372.26	372.27	302	16	R	F	F	<i>Coccolithus pelagicus</i>	
45	4	75-76	374.5	375.25	375.26	302	16	F	F	R	<i>Coccolithus f. braarud</i>	
45	6	75-76	377.5	378.25	378.26	303	15	F	F	F	<i>Coccolithus pelagicus f. braarud</i>	
46	4	69-70	384.08	384.77	384.78	308	19	F	F	R	<i>Coccolithus streckeri</i>	
46	6	67-68	387.08	387.75	387.76	306	23	F	C	R	<i>Cyclicargolithus floridanus</i>	
47	1	74-75	389.2	389.94	389.95	18	302	R	F	F	<i>Dictyococcites bisectus <10</i>	
47	4	78-79	393.7	394.48	394.49	303	17	F	C	F	<i>Dictyococcites bisectus</i>	
47	6	84-85	396.7	397.54	397.55	303	19	F	F	F	<i>Dictyococcites productellus (3-5)</i>	
48	2	71-72	400.2	400.91	400.92	302	21	R	C	F	<i>Dictyococcites scriptae</i>	
48	4	71-72	403.2	403.91	403.92	302	20	R	F	F	<i>Discoaster deflandrei</i>	
48	6	71-72	406.2	406.91	406.92	304	15	P	F	R		
49	3	75-76	411.3	412.05	412.06	306	19	F	F	F		
50	2	75-76	419.4	420.15	420.16	300	16	P	F	R		
50	4	75-76	422.4	423.15	423.16	302	14	R	F	R		
50	6	75-76	425.4	426.15	426.16	322	11	F	C			
51	2	70-71	429	429.7	429.71	301	15	R	R	F		
51	4	70-71	432	432.7	432.71	300	12	R	F	R		
51	6	70-71	435	436.9	436.91	302	15	R	C	R		
51	7	56-57	436.2	436.76	436.77	305	14	F	R			
52	3	75-76	440.1	440.85	440.86	301	18	R	C	F	R	
52	5	68-69	443.1	443.78	443.79	306	10	F	C	F		
52	6	71-72	444.6	445.31	445.32	311	10	R	C	F		
53	1	105-106	446.7	447.75	447.76	308	8	F	C	R		
53	2	75-76	448.2	448.95	448.96	303	16	F	C	F		F
53	4	75-76	451.2	451.95	451.96	304	8	F	F	R		
53	6	76-77	454.17	454.93	454.94	300	15	F	F	F	R	R
54	3	99-100	459.3	460.29	460.3	300	18	R	C	C	R	R
54	4	41-42	460.8	461.21	461.22	302	14	F	C	F		P
54	5	100-101	462.3	463.3	463.31	300	22	R	R	C	F	R
55	1	102-103	465.9	466.92	466.93	304	16		C	C		R
55	2	72-73	467.4	468.12	468.13	303	16	F	F	F		
55	CC	6-7	469.84	469.9	469.91	304	15	R		C	C	R
56	2	75-76	477	477.75	477.76	301	13		R	C	F	R
56	4	74-75	480	480.74	480.75	303	16	F	C			F
56	6	79-80	483	483.79	483.8	302	11	R	C	C		
57	2	72-73	486.6	487.32	487.33	301	11	R	C	F	F	P
57	4	80-81	489.6	490.4	490.41	305	10	F	C	F		
58	3	80-81	496.42	497.22	497.23	301	11		C	F	F	
58	5	75-76	499.42	500.17	500.18	303	13		C	F	C	R
58	7	75-76	502.42	503.17	503.18	303	10	R	C	C		P
59	2	60-61	505.8	506.4	506.41	301	12	R	C	F	F	P
61	2	46-47	524	524.96	524.97	305	14	R	C	F	R	R
62	2	72-73	534.6	535.32	535.33	300	18	R	C	F	R	R

Table 3 - continued

Core	Section	Sample Interval	Core Top Depth (mbsf)				Sample Bottom Depth (mbsf) CSF-A	Total Abundance	Diversity	<i>Emiliania huxleyi</i>	<i>Gephyrocapsa crassippons</i>	<i>Gephyrocapsa crassiprons</i>	<i>Gephyrocapsa caribbeana (3-4)</i>	<i>Gephyrocapsa caribbeana (4-5.5)</i>	<i>Gephyrocapsa caribbeana (>5.5)</i>	<i>Gephyrocapsa oceanica (>6.5)</i>	<i>Gephyrocapsa oceanica (3-4)</i>	<i>Gephyrocapsa oceanica (4-5.5)</i>	<i>Gephyrocapsa oceanica (>5.5)</i>	<i>Gephyrocapsa oceanica (>6.5)</i>	<i>Gephyrocapsa omega</i>	<i>Helicosphaera carteri</i>	<i>Helicosphaera cf. sellii</i>	<i>Helicosphaera sellii</i>	
			Sample Top Depth (mbsf)	Total	Abundance	19																			
44	2	85-86	361.9	362.75	362.76	300	19			C	6	F	R			R	F	R			P			F	
44	4	75-76	364.9	365.65	365.66	305	16				110	C	C	C	F			F	F	R			F		F
44	6	75-76	367.9	368.65	368.66	301	20			C	11	F						F	F	F			F		F
45	2	76-77	371.5	372.26	372.27	302	16			C	52	F	R					F	F	F					
45	4	75-76	374.5	375.25	375.26	302	16			C	38	C					C	F	F	R	C	F		F	
45	6	75-76	377.5	378.25	378.26	303	15			R	43	C	C	C	F		R	R	F				P		
46	4	69-70	384.08	384.77	384.78	308	19			C	47	C	F	F	F		F	F	F	R					
46	6	67-68	387.08	387.75	387.76	306	23			F	111	C	F	C	F		F	R	R			R		R	
47	1	74-75	389.2	389.94	389.95	18	302			C	26	C	R	F				R				R	R		
47	4	78-79	393.7	394.48	394.49	303	17			F	144	C	C	C	F		R	R	F	R		P		F	
47	6	84-85	396.7	397.54	397.55	303	19			C	36	F	R	F	C		R	R	F		R		F		
48	2	71-72	400.2	400.91	400.92	302	21			R	62	C	F	C	C		R	R	R		R		R		
48	4	71-72	403.2	403.91	403.92	302	20			C	21	F	F	F	F		R	R	R	R		R		R	
48	6	71-72	406.2	406.91	406.92	304	15			F	111	C	R	C	C		F	R	R		F		R		
49	3	75-76	411.3	412.05	412.06	306	19			C	70	C	F	C	C	F	F	R	F			F		F	
50	2	75-76	419.4	420.15	420.16	300	16			F	134	C	F	F	R		R	F					R		
50	4	75-76	422.4	423.15	423.16	302	14			C	104	C	F	C	F		R	R	F		R		R		
50	6	75-76	425.4	426.15	426.16	322	11				16	C	A	A				C	C			F		P	
51	2	70-71	429	429.7	429.71	301	15			C	61	C	F	C	F		F	R	R			P			
51	4	70-71	432	432.7	432.71	300	12				75	C	C	C	R										
51	6	70-71	435	436.9	436.91	302	15			C	22	F	C	C			F	F	R			P		R	
51	7	56-57	436.2	436.76	436.77	305	14			F	91	C	C	C			F	R			R		R		
52	3	75-76	440.1	440.85	440.86	301	18			F	114	C	F	F							R		F		
52	5	68-69	443.1	443.78	443.79	306	10				193	A	C	C							F		F		
52	6	71-72	444.6	445.31	445.32	311	10				168	A	C	C							R		R		
53	1	105-106	446.7	447.75	447.76	308	8				52	C	C	C							R		F		
53	2	75-76	448.2	448.95	448.96	303	16			C	78	C	C	C			R	R			P				
53	4	75-76	451.2	451.95	451.96	304	8				14	F	C	C											
53	6	76-77	454.17	454.93	454.94	300	15			C	12	F	F				C								
54	3	99-100	459.3	460.29	460.3	300	18			F	31	F	C	F			R				R		R		
54	4	41-42	460.8	461.21	461.22	302	14			C	92	C	C	C			F				F		F		
54	5	100-101	462.3	463.3	463.31	300	22				19	F	F	F			R				R		R		
55	1	102-103	465.9	466.92	466.93	304	16			F	5	F			R		R				R	R	R		
55	2	72-73	467.4	468.12	468.13	303	16			R	49	C	C	F			R				F		F		
55	CC	6-7	469.84	469.9	469.91	304	15			F	17	F	R								F		F		
56	2	75-76	477	477.75	477.76	301	13			R	6	F	C				F				R		F		
56	4	74-75	480	480.74	480.75	303	16			F	20	C	C	F			C	R			F		F		
56	6	79-80	483	483.79	483.8	302	11										R								
57	2	72-73	486.6	487.32	487.33	301	11				133	C	C									F		F	
57	4	80-81	489.6	490.4	490.41	305	10				24	C	A	F											
58	3	80-81	496.42	497.22	497.23	301	11								R										
58	5	75-76	499.42	500.17	500.18	303	13				4	F	F												
58	7	75-76	502.42	503.17	503.18	303	10				7	F									R		F		
59	2	60-61	505.8	506.4	506.41	301	12				9	F	R	R									F		
61	2	46-47	43	524.96	524.97	305	14				4	R									R		F		
62	2	72-73	534.6	535.32	535.33	300	18			F	6	F	F			R							F		

Table 3 - continued

Core Section	Sample Interval	Core Top Depth (mbsf)		Sample Top Depth (mbsf) CSF-A		Sample Bottom Depth (mbsf) CSF-A		Total Abundance	Diversity
		Core Top Depth (mbsf)	Sample Top Depth (mbsf) CSF-A	Core Top Depth (mbsf)	Sample Top Depth (mbsf) CSF-A	Core Top Depth (mbsf)	Sample Top Depth (mbsf) CSF-A		
44	2	85-86	361.9	362.75	362.76	300	19	R	<i>Pontosphaera discopora</i>
44	4	75-76	364.9	365.65	365.66	305	16	R	<i>Pontosphaera japonica</i>
44	6	75-76	367.9	368.65	368.66	301	20	R	<i>Pontosphaera multipora</i>
45	2	76-77	371.5	372.26	372.27	302	16		<i>Pseudoemiliania lacunosa</i>
45	4	75-76	374.5	375.25	375.26	302	16		<i>Pseudoemiliania ovata</i>
45	6	75-76	377.5	378.25	378.26	303	15	R	<i>Pseudoemiliania pacifica</i>
46	4	69-70	384.08	384.77	384.78	308	19	P	<i>Reticulofenestra amplius</i>
46	6	67-68	387.08	387.75	387.76	306	23	R	<i>Reticulofenestra asanoi</i>
47	1	74-75	389.2	389.94	389.95	18	302	F	<i>Reticulofenestra daviesi</i>
47	4	78-79	393.7	394.48	394.49	303	17		<i>Reticulofenestra dictyoda</i>
47	6	84-85	396.7	397.54	397.55	303	19	R	<i>Reticulofenestra filewiczii</i>
48	2	71-72	400.2	400.91	400.92	302	21		<i>Reticulofenestra gelida</i>
48	4	71-72	403.2	403.91	403.92	302	20		<i>Reticulofenestra hagii (<3)</i>
48	6	71-72	406.2	406.91	406.92	304	15	R	<i>Reticulofenestra hagii (3-5)</i>
49	3	75-76	411.3	412.05	412.06	306	19	F	
50	2	75-76	419.4	420.15	420.16	300	16	P	
50	4	75-76	422.4	423.15	423.16	302	14	R	
50	6	75-76	425.4	426.15	426.16	322	11	F	
51	2	70-71	429	429.7	429.71	301	15		
51	4	70-71	432	432.7	432.71	300	12		
51	6	70-71	435	436.9	436.91	302	15		
51	7	56-57	436.2	436.76	436.77	305	14		
52	3	75-76	440.1	440.85	440.86	301	18	R	
52	5	68-69	443.1	443.78	443.79	306	10		
52	6	71-72	444.6	445.31	445.32	311	10		
53	1	105-106	446.7	447.75	447.76	308	8	P	
53	2	75-76	448.2	448.95	448.96	303	16	R	
53	4	75-76	451.2	451.95	451.96	304	8		
53	6	76-77	454.17	454.93	454.94	300	15		
54	3	99-100	459.3	460.29	460.3	300	18		
54	4	41-42	460.8	461.21	461.22	302	14		
54	5	100-101	462.3	463.3	463.31	300	22	R	
55	1	102-103	465.9	466.92	466.93	304	16		
55	2	72-73	467.4	468.12	468.13	303	16	P	
55	CC	6-7	469.84	469.9	469.91	304	15		
56	2	75-76	477	477.75	477.76	301	13		
56	4	74-75	480	480.74	480.75	303	16	R	
56	6	79-80	483	483.79	483.8	302	11	R	
57	2	72-73	486.6	487.32	487.33	301	11	R	
57	4	80-81	489.6	490.4	490.41	305	10	F	
58	3	80-81	496.42	497.22	497.23	301	11		
58	5	75-76	499.42	500.17	500.18	303	13		
58	7	75-76	502.42	503.17	503.18	303	10		
59	2	60-61	505.8	506.4	506.41	301	12		
61	2	46-47	524.96	524.97	524.97	305	14		
62	2	72-73	534.6	535.32	535.33	300	18		

Table 3 - continued

Core Section	Sample Interval	Core Top Depth (mbsf)	Sample Top Depth (mbsf) CSF-A			Total Abundance	Diversity	<i>Reticulofenestra minuta</i>	<i>Reticulofenestra minutula</i>	<i>Reticulofenestra pseudounbilica</i>	<i>Thoracosphaera sp.</i>	Fields Of View
			Sample Bottom Depth (mbsf) CSF-A	Total Abundance	Diversity							
44	2	85-86	361.9	362.75	362.76	300	19	F		P		29
44	4	75-76	364.9	365.65	365.66	305	16		C			25
44	6	75-76	367.9	368.65	368.66	301		F	F			27
45	2	76-77	371.5	372.26	372.27	302	16	R	R			63
45	4	75-76	374.5	375.25	375.26	302	16					22
45	6	75-76	377.5	378.25	378.26	303	15	F				21
46	4	69-70	384.08	384.77	384.78	308	19					39
46	6	67-68	387.08	387.75	387.76	306	23	R	F			37
47	1	74-75	389.2	389.94	389.95	18	302		F			21
47	4	78-79	393.7	394.48	394.49	303	17	F	R			23
47	6	84-85	396.7	397.54	397.55	303	19	R		R		44
48	2	71-72	400.2	400.91	400.92	302	21	R	R			34
48	4	71-72	403.2	403.91	403.92	302	20	R	R			55
48	6	71-72	406.2	406.91	406.92	304	15	R				28
49	3	75-76	411.3	412.05	412.06	306	19					21
50	2	75-76	419.4	420.15	420.16	300	16		R			47
50	4	75-76	422.4	423.15	423.16	302	14					31
50	6	75-76	425.4	426.15	426.16	322	11		F			9
51	2	70-71	429	429.7	429.71	301	15		R			33
51	4	70-71	432	432.7	432.71	300	12	F	R			49
51	6	70-71	435	436.9	436.91	302	15		R	P		27
51	7	56-57	436.2	436.76	436.77	305	14	F	R			32
52	3	75-76	440.1	440.85	440.86	301	18					38
52	5	68-69	443.1	443.78	443.79	306	10		F			8
52	6	71-72	444.6	445.31	445.32	311	10					11
53	1	105-106	446.7	447.75	447.76	308	8					18
53	2	75-76	448.2	448.95	448.96	303	16					12
53	4	75-76	451.2	451.95	451.96	304	8		R			20
53	6	76-77	454.17	454.93	454.94	300	15	F	R			51
54	3	99-100	459.3	460.29	460.3	300	18	F	R			48
54	4	41-42	460.8	461.21	461.22	302	14	F	F			20
54	5	100-101	462.3	463.3	463.31	300	22		R			91
55	1	102-103	465.9	466.92	466.93	304	16		R			36
55	2	72-73	467.4	468.12	468.13	303	16	F	F			40
55	CC	6-7	469.84	469.9	469.91	304	15	R				50
56	2	75-76	477	477.75	477.76	301	13	R	R			48
56	4	74-75	480	480.74	480.75	303	16		R			18
56	6	79-80	483	483.79	483.8	302	11	R	F	R		57
57	2	72-73	486.6	487.32	487.33	301	11		R			18
57	4	80-81	489.6	490.4	490.41	305	10					6
58	3	80-81	496.42	497.22	497.23	301	11					36
58	5	75-76	499.42	500.17	500.18	303	13		R			31
58	7	75-76	502.42	503.17	503.18	303	10					27
59	2	60-61	505.8	506.4	506.41	301	12					39
61	2	46-47	43	524.96	524.97	305	14	R		R		43
62	2	72-73	534.6	535.32	535.33	300	18	F	R	R		38

Table 4: Raw semi-quantitative calcareous nannofossil abundance counts from Hole U1352B.

Core	Section	Sample Interval	Core Top Depth (mbsf)	Sample Top Depth (mbsf) CSF-A	Sample Bottom Depth (mbsf) CSF-A	Nano Abundance	Preservation	Total Abundance	Diversity		<i>Braunodysphaera bigelowi</i>	<i>Calcidiscus leptopus</i>	<i>Calcidiscus macintyrei</i>	<i>Coccolithus pelagicus</i>	<i>Coccolithus pelagicus f. braarud</i>	<i>Coccolithus streckeri</i>	<i>Cyclicargolithus abisectus</i>	<i>Cyclicargolithus floridanus</i>	<i>Cyclaglosphaera sp.</i>	<i>Dictyococcites bissectus <40</i>	<i>Dictyococcites bissectus</i>
									Core	Section											
12	2	76-77	104.7	105.46	105.47	C	M	303	19		3			20	4	1			3		P
12	6	80-81	110.66	111.46	111.47	A	G	309	14		P			15	1						
13	5	69-70	118.68	119.37	119.38	A-C	G	304	11		1			22	1				3		
14	1	70-71	122.2	122.9	122.91	A-C	G	309	15					12	P	1		20			P
14	5	130-131	128.2	129.5	129.51	A	G	306	18		2			11	3	2					1
15	4	51-52	136.13	136.64	136.65	A	G	303	15		P			18	5						1
16	2	74-75	142.7	143.44	143.45	A	G	305	16					18	17	2				P	
16	6	79-80	148.67	149.46	149.47	VA	G	332	8					19	11	2					
17	4	54-55	154.49	155.03	155.04	A	G	316	12		P			3	1	1	1	1			
18	4	25-26	160.27	160.52	160.53	A	G	309	17		2			9	7	P	P	1			P
19	2	70-71	167.2	167.9	167.91	F	M	100	11					41	10				5		
19	6	27-28	173.17	173.44	173.45	B	-	0	0												
21	2	72-73	181.2	181.92	181.93	A	G	319	9		1				10				1		
22	2	74-75	190.7	191.44	191.45	A	G	340	12		P				17		P	P			
22	5	75-76	195.2	195.95	195.96	VA	G-M	347	6		2				15						
23	2	74-75	200.2	200.94	200.95	C	G	302	8						24				P		1
23	4	75-76	203.2	203.95	203.96	C	M	302	10					27	23			4			
23	6	100-101	206.2	207.2	207.21	A-C	G	311	13		1			22	11			2			P
24	5	63-64	214.2	214.83	214.84	A	G	304	11					8	15			1			
25	3	75-76	220.7	221.45	221.46	C	G	308	13					1	1			P			
25	7	40-41	226.2	226.2	226.61	A	M	303	12					2	1						
26	4	75-76	231.62	232.37	232.38	VA	G	303	8					4	1						
27	2	25-26	238.2	238.45	238.46	VA	G	302	6					4			1				
27	4	55-56	241.2	241.75	241.76	VA	G	322	4		1			9							
27	6	25-26	244.2	244.45	244.46	VA	G	317	9					8	2						
28	2	112-113	247.63	248.75	248.76	A	G	304	12		6			7			2				
28	3	83-84	249.13	249.96	249.97	A	M	302	18		18	1	25	5			2				
28	4	47-48	250.13	250.6	250.61	C	M-P	302	22		3			32	1			17		2	
29	2	100-101	252.7	253.7	253.71	F	M	303	18		3			19			1	40	1		
30	2	89-90	259.2	260.09	260.1	F	G-M	303	17		1			21	1			11			
30	4	89-90	262.2	263.09	263.1	F	G-M	301	22	1	2			52	3		1	40		2	
31	5	113-114	271.01	272.14	272.15	C	G	314	19	1				25	3			6			
32	2	109-110	273.7	274.8	274.81	C	G-M	319	8					16	3			1			
32	4	110-111	276.7	277.79	277.8	A	M	301	11					4				4			
33	2	33-34	283.11	283.44	283.45	C	M	301	6					3	66	3					
33	4	89-90	284.64	285.53	285.54	A	G	303	13		1			7	2			3		1	
33	6	23-24	287.62	287.85	287.86	A-C	M	301	7					16	5		1	4			
34	2	100-101	288.46	289.46	289.47	A	G-M	301	12		2						P			P	
34	4	14-15	290.77	290.91	290.92	A	G-M	304	8		2			6	1			5			
35	2	46-47	294.34	294.8	294.81	A	G	309	11		2			11	4			1			
36	2	14-15	296.5	296.64	296.65	F	M	305	10		4							2			
38	2	75-76	304.1	304.85	304.86	C	M	302	12		7			13				1			
38	6	35-36	310.1	310.45	310.46	F	G	301	13		2			11	2			2			
39	4	79-80	316.7	317.49	317.5	F	M	301	14	1	15			30	1			3			
40	1	105-106	321.9	322.95	322.96	F	G	304	13		1			4				1		1	
40	2	75-76	323.4	324.15	324.16	C	G-M	304	7		4			25	2						
40	3	105-106	324.9	325.95	325.96	A	M	319	14		8			37	1			2			
40	4	75-76	326.4	327.15	327.16	C	M	303	15		3			3				2			P
41	2	75-76	333	333.75	333.76	C	M	300	13		22			52	8			3			
41	4	61-62	336	336.61	336.62	C	G-M	303	20	P	8			85	13	1		2		3	
41	6	69-70	339	339.69	339.7	F-C	G	311	17		2			90	29			5			
42	1	80-81	341.1	341.9	341.91	F	P	302	17		2			9	1			P			
42	3	80-81	344.1	344.9	344.91	F	G	301	20		4			2				1		15	
42	4	79-80	345.6	346.39	346.4	F	G	306	18		11			3	1			1			
43	2	75-76	352.2	352.95	352.96	F	G-M	304	18		5			14	5			6		4	
43	3	75-76	353.7	354.45	354.46	C	G	300	16		2			4	1						
43	5	75-76	356.7	357.45	357.46	A	G	303	25	1	3			4						2	
43	7	45-46	359.2	359.65	359.66	A	G	304	17		6			6	1			2			

Table 4 - continued

Core	Section	Sample Interval	Core Top Depth (mbsf)	Sample Top Depth (mbsf) CSF-A	Sample Bottom Depth (mbsf) CSF-A	Nano Abundance	Preservation	Total Abundance	Diversity	Dictyococcites productus/lus (3-5)	Dictyococcites scriptae	Discoaster deflandrei	Emiliania huxleyi	Gephyrocapsa aperta	Gephyrocapsa crassipons	Gephyrocapsa caribbeanca (3-4)	Gephyrocapsa caribbeanca (4-5.5)	Gephyrocapsa caribbeanca (>5.5)	Gephyrocapsa oceanica (3-4)
12	2	76-77	104.7	105.46	105.47	C	M	303	19	2		P	10	128	3	12		87	
12	6	80-81	110.66	111.46	111.47	A	G	309	14			P	3	206				53	
13	5	69-70	118.68	119.37	119.38	A-C	G	304	11					17		3		228	
14	1	70-71	122.2	122.9	122.91	A-C	G	309	15					17		18		215	
14	5	130-131	128.2	129.5	129.51	A	G	306	18	1				63	1	16		151	
15	4	51-52	136.13	136.64	136.65	A	G	303	15	1				11	1	9		192	
16	2	74-75	142.7	143.44	143.45	A	G	305	16	9				18	1	22		123	
16	6	79-80	148.67	149.46	149.47	VA	G	332	8							15		272	
17	4	54-55	154.49	155.03	155.04	A	G	316	12							8		281	
18	4	25-26	160.27	160.52	160.53	A	G	309	17					61		39	4	158	
19	2	70-71	167.2	167.9	167.91	F	M	100	11			1		10					
19	6	27-28	173.17	173.44	173.45	B	—	0	0										
21	2	72-73	181.2	181.92	181.93	A	G	319	9					199	15	3		7	
22	2	74-75	190.7	191.44	191.45	A	G	340	12					245		4		1	
22	5	75-76	195.2	195.95	195.96	VA	G-M	347	6					312		2		6	
23	2	74-75	200.2	200.94	200.95	C	G	302	8						181			53	
23	4	75-76	203.2	203.95	203.96	C	M	302	10			P		2	197	1			
23	6	100-101	206.2	207.2	207.21	A-C	G	311	13					59	200			5	
24	5	63-64	214.2	214.83	214.84	A	G	304	11	1	1			41	226	1			
25	3	75-76	220.7	221.45	221.46	C	G	308	13			P		54	241	1			
25	7	40-41	226.2	226.6	226.61	A	M	303	12	8				67	178	34		4	
26	4	75-76	231.62	232.37	232.38	VA	G	303	8					291					
27	2	25-26	238.2	238.45	238.46	VA	G	302	6					287	7			2	
27	4	55-56	241.2	241.75	241.76	VA	G	322	4					310				2	
27	6	25-26	244.2	244.45	244.46	VA	G	317	9					290	2			6	
28	2	112-113	247.63	248.75	248.76	A	G	304	12					244		1		9	
28	3	83-84	249.13	249.96	249.97	A	M	302	18					205	3	2		10	
28	4	47-48	250.13	250.6	250.61	C	M-P	302	22					192	2	4	2	4	
29	2	100-101	252.7	253.7	253.71	F	M	303	18			1	1	188	1	5		8	
30	2	89-90	259.2	260.09	260.1	F	G-M	303	17					229	4	4		2	
30	4	89-90	262.2	263.09	263.1	F	G-M	301	22					124	18	8		3	
31	5	113-114	271.01	272.14	272.15	C	G	314	19			1		217	13	1		1	
32	2	109-110	273.7	274.8	274.81	C	G-M	319	8					285					
32	4	110-111	276.7	277.79	277.8	A	M	301	11					230	15	9		14	
33	2	33-34	283.11	283.44	283.45	C	M	301	6						225				
33	4	89-90	284.64	285.53	285.54	A	G	303	13					277	1				
33	6	23-24	287.62	287.85	287.86	A-C	M	301	7					271				3	
34	2	100-101	288.46	289.46	289.47	A	G-M	301	12					285					
34	4	14-15	290.77	290.91	290.92	A	G-M	304	8					283				1	
35	2	46-47	294.34	294.8	294.81	A	G	309	11					275	1			8	
36	2	14-15	296.5	296.64	296.65	F	M	305	10			1		289		1			
38	2	75-76	304.1	304.85	304.86	C	M	302	12					244	7	3		2	
38	6	35-36	310.1	310.45	310.46	F	G	301	13					267	3	2		1	
39	4	79-80	316.7	317.49	317.5	F	M	301	14					206	4	3			
40	1	105-106	321.9	322.95	322.96	F	G	304	13					261	21	1		2	
40	2	75-76	323.4	324.15	324.16	C	G-M	304	7					256					
40	3	105-106	324.9	325.95	325.96	A	M	319	14					180	8	9		7	
40	4	75-76	326.4	327.15	327.16	C	M	303	15					247		4		12	
41	2	75-76	333	333.75	333.76	C	M	300	13					145	28		1	1	
41	4	61-62	336	336.61	336.62	C	G-M	303	20	4				140	19	2			
41	6	69-70	339	339.69	339.7	F-C	G	311	17			1		66	72	7			
42	1	80-81	341.1	341.9	341.91	F	P	302	17	1				188	76	1			
42	3	80-81	344.1	344.9	344.91	F	G	301	20					154	45	7		1	
42	4	79-80	345.6	346.39	346.4	F	G	306	18					98	105	6	6	1	
43	2	75-76	352.2	352.95	352.96	F	G-M	304	18	2	2			234	17		1	3	
43	3	75-76	353.7	354.45	354.46	C	G	300	16					125	32	7	4	25	
43	5	75-76	356.7	357.45	357.46	A	G	303	25	1	7			42	80	5	5	24	
43	7	45-46	359.2	359.65	359.66	A	G	304	17					71	49	18	67	5	

Table 4 - continued

Core	Section	Sample Interval	Core Top Depth (mbsf)	Sample Top Depth (mbsf) CSF-A	Sample Bottom Depth (mbsf) CSF-A	Nanno Abundance	Preservation	Total Abundance	Diversity	<i>Gephyrocapsa oceanica</i> (>5.5)	<i>Gephyrocapsa oceanica</i> (>5.5)	<i>Gephyrocapsa oceanica</i> (>6.5)	<i>Gephyrocapsa omega</i>	<i>Helicosphaera carteri</i>	<i>Helicosphaera cf sellii</i>	<i>Helicosphaera sellii</i>	<i>Pontosphaera discopora</i>	<i>Pontosphaera japonica</i>	<i>Pontosphaera multipora</i>	<i>Pseudoemiliania lacunosa</i>
12	2	76-77	104.7	105.46	105.47	C	M	303	19					P						
12	6	80-81	110.66	111.46	111.47	A	G	309	14					P						
13	5	69-70	118.68	119.37	119.38	A-C	G	304	11					1						
14	1	70-71	122.2	122.9	122.91	A-C	G	309	15					P						
14	5	130-131	128.2	129.5	129.51	A	G	306	18					P						
15	4	51-52	136.13	136.64	136.65	A	G	303	15											
16	2	74-75	142.7	143.44	143.45	A	G	305	16	1				P						
16	6	79-80	148.67	149.46	149.47	VA	G	332	8					P						
17	4	54-55	154.49	155.03	155.04	A	G	316	12					1						
18	4	25-26	160.27	160.52	160.53	A	G	309	17					2					1	
19	2	70-71	167.2	167.9	167.91	F	M	100	11											
19	6	27-28	173.17	173.44	173.45	B	-	0	0											
21	2	72-73	181.2	181.92	181.93	A	G	319	9											
22	2	74-75	190.7	191.44	191.45	A	G	340	12					P						
22	5	75-76	195.2	195.95	195.96	VA	G-M	347	6											
23	2	74-75	200.2	200.94	200.95	C	G	302	8					31						
23	4	75-76	203.2	203.95	203.96	C	M	302	10					17						
23	6	100-101	206.2	207.2	207.21	A-C	G	311	13					1						
24	5	63-64	214.2	214.83	214.84	A	G	304	11					5						
25	3	75-76	220.7	221.45	221.46	C	G	308	13					P						
25	7	40-41	226.2	226.6	226.61	A	M	303	12					2						
26	4	75-76	231.62	232.37	232.38	VA	G	303	8										1	
27	2	25-26	238.2	238.45	238.46	VA	G	302	6											
27	4	55-56	241.2	241.75	241.76	VA	G	322	4											
27	6	25-26	244.2	244.45	244.46	VA	G	317	9				4	2					1	
28	2	112-113	247.63	248.75	248.76	A	G	304	12				22						2	
28	3	83-84	249.13	249.96	249.97	A	M	302	18	1			5						3	
28	4	47-48	250.13	250.6	250.61	C	M-P	302	22				3	1						
29	2	100-101	252.7	253.7	253.71	F	M	303	18				3						1	
30	2	89-90	259.2	260.09	260.1	F	G-M	303	17				2	2						
30	4	89-90	262.2	263.09	263.1	F	G-M	301	22				1	1					1	1
31	5	113-114	271.01	272.14	272.15	C	G	314	19	1										
32	2	109-110	273.7	274.8	274.81	C	G-M	319	8				1						3	
32	4	110-111	276.7	277.79	277.8	A	M	301	11											
33	2	33-34	283.11	283.44	283.45	C	M	301	6										3	
33	4	89-90	284.64	285.53	285.54	A	G	303	13										1	
33	6	23-24	287.62	287.85	287.86	A-C	M	301	7											
34	2	100-101	288.46	289.46	289.47	A	G-M	301	12					1						2
34	4	14-15	290.77	290.91	290.92	A	G-M	304	8					3						3
35	2	46-47	294.34	294.8	294.81	A	G	309	11					2						
36	2	14-15	296.64	296.64	296.65	F	M	305	10										1	
38	2	75-76	304.1	304.85	304.86	C	M	302	12	1									5	
38	6	35-36	310.1	310.45	310.46	F	G	301	13										1	1
39	4	79-80	316.7	317.49	317.5	F	M	301	14										10	
40	1	105-106	321.9	322.95	322.96	F	G	304	13	1										1
40	2	75-76	323.4	324.15	324.16	C	G-M	304	7											
40	3	105-106	324.9	325.95	325.96	A	M	319	14	1									13	
40	4	75-76	326.4	327.15	327.16	C	M	303	15					1					P	
41	2	75-76	333	333.75	333.76	C	M	300	13										3	2
41	4	61-62	336	336.61	336.62	C	G-M	303	20										2	1
41	6	69-70	339	339.69	339.7	F-C	G	311	17		1								4	5
42	1	80-81	341.1	341.9	341.91	F	P	302	17										7	
42	3	80-81	344.1	344.9	344.91	F	G	301	20										5	1
42	4	79-80	345.6	346.39	346.4	F	G	306	18	2			1	1					2	6
43	2	75-76	352.2	352.95	352.96	F	G-M	304	18	1									1	
43	3	75-76	353.7	354.45	354.46	C	G	300	16	13			28						1	7
43	5	75-76	356.7	357.45	357.46	A	G	303	25	1	4	33							1	1
43	7	45-46	359.2	359.65	359.66	A	G	304	17	24									2	9

Table 4 - continued

Core	Section	Sample Interval	Core Top Depth (mbsf)	Sample Top Depth (mbsf) CSF-A	Sample Bottom Depth (mbsf) CSF-A	Nanno Abundance	Preservation	Total Abundance	Diversity	<i>Pseudoeumiliania ovata</i>	<i>Pseudoeumiliania pacifica</i>	<i>Reticulofenestra amplis</i>	<i>Reticulofenestra asanoi</i>	<i>Reticulofenestra daviesi</i>	<i>Reticulofenestra dictyoda</i>	<i>Reticulofenestra filewiczi</i>	<i>Reticulofenestra gelida</i>	<i>Reticulofenestra haqii (<2)</i>	<i>Reticulofenestra haqii (3-5)</i>	<i>Reticulofenestra minuta</i>
12	2	76-77	104.7	105.46	105.47	C	M	303	19		4							1	19	
12	6	80-81	110.66	111.46	111.47	A	G	309	14		3						P	4	6	
13	5	69-70	118.68	119.37	119.38	A-C	G	304	11					1	P			27		
14	1	70-71	122.2	122.9	122.91	A-C	G	309	15		P		P	1				23		
14	5	130-131	128.2	129.5	129.51	A	G	306	18		1					P	38	10	2	
15	4	51-52	136.13	136.64	136.65	A	G	303	15	1	1					P	5		56	
16	2	74-75	142.7	143.44	143.45	A	G	305	16							P	4	1	71	
16	6	79-80	148.67	149.46	149.47	VA	G	332	8							1	8	4	4	
17	4	54-55	154.49	155.03	155.04	A	G	316	12				P					12		
18	4	25-26	160.27	160.52	160.53	A	G	309	17								14	3	6	
19	2	70-71	167.2	167.9	167.91	F	M	100	11				2	4	7	13	1			
19	6	27-28	173.17	173.44	173.45	B	-	0	0											
21	2	72-73	181.2	181.92	181.93	A	G	319	9										82	
22	2	74-75	190.7	191.44	191.45	A	G	340	12		P								70	
22	5	75-76	195.2	195.95	195.96	VA	G-M	347	6										10	
23	2	74-75	200.2	200.94	200.95	C	G	302	8		P								12	
23	4	75-76	203.2	203.95	203.96	C	M	302	10											
23	6	100-101	206.2	207.2	207.21	A-C	G	311	13					1	P	5	4			
24	5	63-64	214.2	214.83	214.84	A	G	304	11					1	1	1		3		
25	3	75-76	220.7	221.45	221.46	C	G	308	13		P			2				7		
25	7	40-41	226.2	226.6	226.61	A	M	303	12					2		3	1	1		
26	4	75-76	231.62	232.37	232.38	VA	G	303	8	2				1	1			2		
27	2	25-26	238.2	238.45	238.46	VA	G	302	6									1		
27	4	55-56	241.2	241.75	241.76	VA	G	322	4										2	
27	6	25-26	244.2	244.45	244.46	VA	G	317	9											
28	2	112-113	247.63	248.75	248.76	A	G	304	12	1							2	7		
28	3	83-84	249.13	249.96	249.97	A	M	302	18	8							4	2	4	
28	4	47-48	250.13	250.6	250.61	C	M-P	302	22	1				2	4	10	4	14		
29	2	100-101	252.7	253.7	253.71	F	M	303	18			6		2			12		9	
30	2	89-90	259.2	260.09	260.1	F	G-M	303	17			1		2	2	11	2	7		
30	4	89-90	262.2	263.09	263.1	F	G-M	301	22			1	6	2		21	8	4		
31	5	113-114	271.01	272.14	272.15	C	G	314	19	2			1	2	2	17	3	16		
32	2	109-110	273.7	274.8	274.81	C	G-M	319	8					5					5	
32	4	110-111	276.7	277.79	277.8	A	M	301	11				1		1	14	2	7		
33	2	33-34	283.11	283.44	283.45	C	M	301	6					3		2	3	1		
33	4	89-90	284.64	285.53	285.54	A	G	303	13									1		
33	6	23-24	287.62	287.85	287.86	A-C	M	301	7											
34	2	100-101	288.46	289.46	289.47	A	G-M	301	12	3				3			2	1		
34	4	14-15	290.77	290.91	290.92	A	G-M	304	8									11		
35	2	46-47	294.34	294.8	294.81	A	G	309	11	2		1						2		
36	2	14-15	296.5	296.64	296.65	F	M	305	10	2						1	3			
38	2	75-76	304.1	304.85	304.86	C	M	302	12	4							14			
38	6	35-36	310.1	310.45	310.46	F	G	301	13								1	7	1	
39	4	79-80	316.7	317.49	317.5	F	M	301	14	14							1	11		
40	1	105-106	321.9	322.95	322.96	F	G	304	13								1	8		
40	2	75-76	323.4	324.15	324.16	C	G-M	304	7	8					1					
40	3	105-106	324.9	325.95	325.96	A	M	319	14	16							33			
40	4	75-76	326.4	327.15	327.16	C	M	303	15	12			4		4		2	8		
41	2	75-76	333	333.75	333.76	C	M	300	13	13								20		
41	4	61-62	336	336.61	336.62	C	G-M	303	20	10			3	P	2	5	1			
41	6	69-70	339	339.69	339.7	F-C	G	311	17	1				4		4	20			
42	1	80-81	341.1	341.9	341.91	F	P	302	17	5	1	1		4		1	2	3		
42	3	80-81	344.1	344.9	344.91	F	G	301	20	18		1		3		8	22	1		
42	4	79-80	345.6	346.39	346.4	F	G	306	18	12							45	1		
43	2	75-76	352.2	352.95	352.96	F	G-M	304	18	1			1		2		4			
43	3	75-76	353.7	354.45	354.46	C	G	300	16								1	40		
43	5	75-76	356.7	357.45	357.46	A	G	303	25	19			3			8	40	1		
43	7	45-46	359.2	359.65	359.66	A	G	304	17	10			2			1	23			

Table 4 - continued

Core	Section	Sample Interval	Core Top Depth (mbsf)			Sample Top Depth (mbsf) CSF-A			Sample Bottom Depth (mbsf) CSF-A			Diversity	<i>Reticulofenestra minutula</i>	<i>Reticulofenestra pseudoumbilicalis</i>	<i>Thoracosphaera</i> sp.	Fields Of View
			104.7	105.46	105.47	C	M	303	19	6	P					
12	2	76-77	104.7	105.46	105.47	A	G	309	14	7					5	
12	6	80-81	110.66	111.46	111.47	A-C	G	304	11						17	
13	5	69-70	118.68	119.37	119.38	A-C	G	309	15	2					10	
14	1	70-71	122.2	122.9	122.91	A-C	G	309	18	4					10	
14	5	130-131	128.2	129.5	129.51	A	G	306	15	2					13	
15	4	51-52	136.13	136.64	136.65	A	G	303	15						8	
16	2	74-75	142.7	143.44	143.45	A	G	305	16	18					5	
16	6	79-80	148.67	149.46	149.47	VA	G	332	8						9	
17	4	54-55	154.49	155.03	155.04	A	G	316	12	7					17	
18	4	25-26	160.27	160.52	160.53	A	G	309	17	2					13	
19	2	70-71	167.2	167.9	167.91	F	M	100	11	6					100	
19	6	27-28	173.17	173.44	173.45	B	-	0	0							
21	2	72-73	181.2	181.92	181.93	A	G	319	9	1					7	
22	2	74-75	190.7	191.44	191.45	A	G	340	12	3					4	
22	5	75-76	195.2	195.95	195.96	VA	G-M	347	6						3	
23	2	74-75	200.2	200.94	200.95	C	G	302	8						25	
23	4	75-76	203.2	203.95	203.96	C	M	302	10		P				31	
23	6	100-101	206.2	207.2	207.21	A-C	G	311	13						22	
24	5	63-64	214.2	214.83	214.84	A	G	304	11						22	
25	3	75-76	220.7	221.45	221.46	C	G	308	13	1	P				10	
25	7	40-41	226.2	226.6	226.61	A	M	303	12						13	
26	4	75-76	231.62	232.37	232.38	VA	G	303	8		P				2	
27	2	25-26	238.2	238.45	238.46	VA	G	302	6						3	
27	4	55-56	241.2	241.75	241.76	VA	G	322	4						2	
27	6	25-26	244.2	244.45	244.46	VA	G	317	9						1	
28	2	112-113	247.63	248.75	248.76	A	G	304	12	1					9	
28	3	83-84	249.13	249.96	249.97	A	M	302	18						16	
28	4	47-48	250.13	250.6	250.61	C	M-P	302	22	1	2				40	
29	2	100-101	252.7	253.7	253.71	F	M	303	18						49	
30	2	89-90	259.2	260.09	260.1	F	G-M	303	17						39	
30	4	89-90	262.2	263.09	263.1	F	G-M	301	22		1				63	
31	5	113-114	271.01	272.14	272.15	C	G	314	19	1	1				18	
32	2	109-110	273.7	274.8	274.81	C	G-M	319	8						8	
32	4	110-111	276.7	277.79	277.8	A	M	301	11						36	
33	2	33-34	283.11	283.44	283.45	C	M	301	6						9	
33	4	89-90	284.64	285.53	285.54	A	G	303	13		1				6	
33	6	23-24	287.62	287.85	287.86	A-C	M	301	7						7	
34	2	100-101	288.46	289.46	289.47	A	G-M	301	12	1					4	
34	4	14-15	290.77	290.91	290.92	A	G-M	304	8						8	
35	2	46-47	294.34	294.8	294.81	A	G	309	11						10	
36	2	14-15	296.5	296.64	296.65	F	M	305	10						12	
38	2	75-76	304.1	304.85	304.86	C	M	302	12	1					26	
38	6	35-36	310.1	310.45	310.46	F	G	301	13						35	
39	4	79-80	316.7	317.49	317.5	F	M	301	14		1				27	
40	1	105-106	321.9	322.95	322.96	F	G	304	13	1					35	
40	2	75-76	323.4	324.15	324.16	C	G-M	304	7						19	
40	3	105-106	324.9	325.95	325.96	A	M	319	14	3					9	
40	4	75-76	326.4	327.15	327.16	C	M	303	15	1					25	
41	2	75-76	333	333.75	333.76	C	M	300	13	2					27	
41	4	61-62	336	336.61	336.62	C	G-M	303	20	2					26	
41	6	69-70	339	339.69	339.7	F-C	G	311	17	2	1				36	
42	1	80-81	341.1	341.9	341.91	F	P	302	17						48	
42	3	80-81	344.1	344.9	344.91	F	G	301	20	1					26	
42	4	79-80	345.6	346.39	346.4	F	G	306	18	4					26	
43	2	75-76	352.2	352.95	352.96	F	G-M	304	18		1				41	
43	3	75-76	353.7	354.45	354.46	C	G	300	16	1					44	
43	5	75-76	356.7	357.45	357.46	A	G	303	25	3					13	
43	7	45-46	359.2	359.65	359.66	A	G	304	17	8					17	

Table 4 - continued

Core	Section	Sample Interval	Core Top Depth (mbsf)	Sample Top Depth (mbsf) CSF-A	Sample Bottom Depth (mbsf) CSF-A	Nanno Abundance	Preservation	Total Abundance	Diversity	<i>Braarudosphaera bigelowii</i>	<i>Calcidiscus leptoporus</i>	<i>Calcidiscus macintyrei</i>	<i>Coccolithus pelagicus</i>	<i>Coccolithus streckeri</i>	<i>Cyclicargolithus abisectus</i>	<i>Cyclicargolithus floridanus</i>	<i>Cyclagelosphaera sp.</i>	<i>Dictyococites bisectus <1.0</i>	<i>Dictyococites bisectus</i>
44	2	85-86	361.9	362.75	362.76	C	G	300	19	1	6	15	1						
44	4	75-76	364.9	365.65	365.66	C	G	305	16		5	6							
44	6	75-76	367.9	368.65	368.66	C	G	301	20		7	3	3				3		
45	2	76-77	371.5	372.26	372.27	C	M	302	16		3	14	3				4		
45	4	75-76	374.5	375.25	375.26	A	G	302	16		4	12	2				2		
45	6	75-76	377.5	378.25	378.26	A	G	303	15		3	14	9						
46	4	69-70	384.08	384.77	384.78	C	G-M	308	19		5	9	3			2	2		
46	6	67-68	387.08	387.75	387.76	F	G	306	23		6	41	3				1		
47	1	74-75	389.2	389.94	389.95	C	M-G	302	18		1	15	6		P				
47	4	78-79	393.7	394.48	394.49	C	G	303	17		3	32	8						
47	6	84-85	396.7	397.54	397.55	C	G	303	19			33	6						
48	2	71-72	400.2	400.91	400.92	C	G-M	302	21		1	70	6			2			
48	4	71-72	403.2	403.91	403.92	F	G	302	20		2	45	12			4			
48	6	71-72	406.2	406.91	406.92	C	G	304	15			19	1						
49	3	75-76	411.3	412.05	412.06	A	G	306	19		3	13	6						
50	2	75-76	419.4	420.15	420.16	C	G	300	16			25	3						
50	4	75-76	422.4	423.15	423.16	A	P	302	14		1	22	3						
50	6	75-76	425.4	426.15	426.16	A	M	322	11		3	12							
51	2	70-71	429	429.7	429.71	C	G	301	15	1	1	16	3						
51	4	70-71	432	432.7	432.71	F	M	300	12		1	29	1						
51	6	70-71	435	436.9	436.91	C-F	G	302	15		1	35	2			2			
51	7	56-57	436.2	436.76	436.77	C	M	305	14			18	3						
52	3	75-76	440.1	440.85	440.86	C	G	301	18		2	76	29	2		2			
52	5	68-69	443.1	443.78	443.79	A	G	306	10		4	10	1						
52	6	71-72	444.6	445.31	445.32	C	G	311	10		1	36	5						
53	1	105-106	446.7	447.75	447.76	C	P	308	8		3	50	1						
53	2	75-76	448.2	448.95	448.96	A	M-P	303	16		3	44	5				5		
53	4	75-76	451.2	451.95	451.96	A	P	304	8		4	18	1						
53	6	76-77	454.17	454.93	454.94	F	G	300	15		6	42	19	1	1		1		
54	3	99-100	459.3	460.29	460.3	C	G	300	18		2	62	55					1	
54	4	41-42	460.8	461.21	461.22	C	M	302	14		11	24	7					2	
54	5	100-101	462.3	463.3	463.31	C	M	300	22		1	97	24			2		2	
55	1	102-103	465.9	466.92	466.93	C	M	304	16			161	71						
55	2	72-73	467.4	468.12	468.13	C	G	303	16		15	25	6						
55	CC	6-7	469.84	469.9	469.91	C	G	304	15	1		89	108	4	2				
56	2	75-76	477	477.75	477.76	C	M-P	301	13			1	99	20		1			
56	4	74-75	480	480.74	480.75	A	P	303	16		3	68					2		
56	6	79-80	483	483.79	483.8	C	M	302	11		1	133	103						
57	2	72-73	486.6	487.32	487.33	C	G	301	11		1	63	8	7					
57	4	80-81	489.6	490.4	490.41	A	M	305	10		1	16	1						
58	3	80-81	496.42	497.22	497.23	C	G	301	11			220	31	24					
58	5	75-76	499.42	500.17	500.18	C	M	303	13			159	14	97	3		2		
58	7	75-76	502.42	503.17	503.18	C	G-M	303	10		1	174	44	56					
59	2	60-61	505.8	506.4	506.41	C	G	301	12		1	219	12	33			1		
61	2	46-47	43	524.96	524.97	C	M	305	14		2	246	11	2		2		2	
62	2	72-73	534.6	535.32	535.33	C	G	300	18		3	146	7	1					

Table 4 - continued

Core	Section	Sample Interval	Core Top Depth (mbsf)	Sample Top Depth (mbsf) CSF-A	Sample Bottom Depth (mbsf) CSF-A	Nanno Abundance	Preservation	Total Abundance	Diversity	<i>Dictyococcites productellus</i> (3-5)	<i>Dictyococcites scriptosae</i>	<i>Discoaster deflandrei</i>	<i>Emiliania huxleyi</i>	<i>Gephyrocapsa aperta</i>	<i>Gephyrocapsa crassipons</i>	<i>Gephyrocapsa caribbeanica</i> (3-4)	<i>Gephyrocapsa caribbeanica</i> (4-5.5)	<i>Gephyrocapsa caribbeanica</i> (>5.5)	<i>Gephyrocapsa caribbeanica</i> (>6.5)	<i>Gephyrocapsa oceanica</i> (3-4)	
44	2	85-86	361.9	362.75	362.76	C	G	300	19					124	6	1			22		
44	4	75-76	364.9	365.65	365.66	C	G	305	16					110	32	38	10		1		
44	6	75-76	367.9	368.65	368.66	C	G	301	20					144	11				10		
45	2	76-77	371.5	372.26	372.27	C	M	302	16					167	52	1			7		
45	4	75-76	374.5	375.25	375.26	A	G	302	16					105	38			65	11	5	
45	6	75-76	377.5	378.25	378.26	A	G	303	15					2	43	54	150	12	1	2	
46	4	69-70	384.08	384.77	384.78	C	G-M	308	19					144	47	8	7	26	6		
46	6	67-68	387.08	387.75	387.76	F	G	306	23					15	111	23	41	10		6	
47	1	74-75	389.2	389.94	389.95	C	M-G	302	18					203	26	2	7				
47	4	78-79	393.7	394.48	394.49	C	G	303	17					7	144	26	50	6	1	1	
47	6	84-85	396.7	397.54	397.55	C	G	303	19					61	36	3	32	86	1	2	
48	2	71-72	400.2	400.91	400.92	C	G-M	302	21					3	62	7	53	80	1	1	
48	4	71-72	403.2	403.91	403.92	F	G	302	20					100	21	11	34	38	2	3	
48	6	71-72	406.2	406.91	406.92	C	G	304	15					3	111	1	57	73			
49	3	75-76	411.3	412.05	412.06	A	G	306	19					52	70	9	33	84	6	4	
50	2	75-76	419.4	420.15	420.16	C	G	300	16					5	134	43	44	3		1	
50	4	75-76	422.4	423.15	423.16	A	P	302	14					95	104	8	34	22		2	
50	6	75-76	425.4	426.15	426.16	A	M	322	11						16	105	140			11	
51	2	70-71	429	429.7	429.71	C	G	301	15					77	61	14	105	6		6	
51	4	70-71	432	432.7	432.71	F	M	300	12					75	99	77	1				
51	6	70-71	435	436.9	436.91	C-F	G	302	15					86	22	34	85			18	
51	7	56-57	436.2	436.76	436.77	C	M	305	14					19	91	113	34			8	
52	3	75-76	440.1	440.85	440.86	C	G	301	18					7	114	32	15				
52	5	68-69	443.1	443.78	443.79	A	G	306	10						193	80	13				
52	6	71-72	444.6	445.31	445.32	C	G	311	10						168	16	80				
53	1	105-106	446.7	447.75	447.76	C	P	308	8						52	135	65				
53	2	75-76	448.2	448.95	448.96	A	M-P	303	16					45	78	46	59			1	
53	4	75-76	451.2	451.95	451.96	A	P	304	8					14	143	122					
53	6	76-77	454.17	454.93	454.94	F	G	300	15					101	12	36				57	
54	3	99-100	459.3	460.29	460.3	C	G	300	18					7	31	97	10			13	
54	4	41-42	460.8	461.21	461.22	C	M	302	14					72	92	29				16	
54	5	100-101	462.3	463.3	463.31	C	M	300	22	1					19	17	38				
55	1	102-103	465.9	466.92	466.93	C	M	304	16						5	5	1				1
55	2	72-73	467.4	468.12	468.13	C	G	303	16					1	49	131	34			2	
55	CC	6-7	469.84	469.9	469.91	C	G	304	15					41	17	3					
56	2	75-76	477	477.75	477.76	C	M-P	301	13					3	6	96				18	
56	4	74-75	480	480.74	480.75	A	P	303	16					11	20	143	10			26	
56	6	79-80	483	483.79	483.8	C	M	302	11											2	
57	2	72-73	486.6	487.32	487.33	C	G	301	11						133	81					
57	4	80-81	489.6	490.4	490.41	A	M	305	10					24	255	1					
58	3	80-81	496.42	497.22	497.23	C	G	301	11									2			
58	5	75-76	499.42	500.17	500.18	C	M	303	13						4	5					
58	7	75-76	502.42	503.17	503.18	C	G-M	303	10						7						
59	2	60-61	505.8	506.4	506.41	C	G	301	12						9	1	1				
61	2	46-47	43	524.96	524.97	C	M	305	14	1						4					
62	2	72-73	534.6	535.32	535.33	C	G	300	18					7	6	8				1	

Table 4 - continued

Core	Section	Sample Interval	Core Top Depth (mbsf)	Sample Top Depth (mbsf) CSF-A	Sample Bottom Depth (mbsf) CSF-A	Nanno Abundance	Preservation	Total Abundance	Diversity	<i>Gephyrocapsa oceanica</i> (4-5.5)	<i>Gephyrocapsa oceanica</i> (>5.5)	<i>Gephyrocapsa omega</i>	<i>Helicosphaera carteri</i>	<i>Helicosphaera cf sellii</i>	<i>Helicosphaera sellii</i>	<i>Pontosphaera discopora</i>	<i>Pontosphaera japonica</i>	<i>Pontosphaera multipora</i>	<i>Pseudoeumiliinia lacunosa</i>
44	2	85-86	361.9	362.75	362.76	C	G	300	19	4	7	37		1				6	
44	4	75-76	364.9	365.65	365.66	C	G	305	16	5	1			3	4	1			
44	6	75-76	367.9	368.65	368.66	C	G	301	20	3	21	21		3	6	1		8	
45	2	76-77	371.5	372.26	372.27	C	M	302	16		24	9						2	
45	4	75-76	374.5	375.25	375.26	A	G	302	16	2	32	13	5						
45	6	75-76	377.5	378.25	378.26	A	G	303	15	7						1			
46	4	69-70	384.08	384.77	384.78	C	G-M	308	19	5	4	1						6	
46	6	67-68	387.08	387.75	387.76	F	G	306	23	2	1		2	1	2	1			
47	1	74-75	389.2	389.94	389.95	C	M-G	302	18	1				1	1	5			
47	4	78-79	393.7	394.48	394.49	C	G	303	17	3	1				7				
47	6	84-85	396.7	397.54	397.55	C	G	303	19		5		4	9	1			5	
48	2	71-72	400.2	400.91	400.92	C	G-M	302	21		2				1			2	
48	4	71-72	403.2	403.91	403.92	F	G	302	20	1	1			1	4			3	
48	6	71-72	406.2	406.91	406.92	C	G	304	15				4	2	1			3	
49	3	75-76	411.3	412.05	412.06	A	G	306	19	1	4		3	4	4			1	
50	2	75-76	419.4	420.15	420.16	C	G	300	16	6				2	1				
50	4	75-76	422.4	423.15	423.16	A	P	302	14	1	5		1	3		1			
50	6	75-76	425.4	426.15	426.16	A	M	322	11	19			1			1			
51	2	70-71	429	429.7	429.71	C	G	301	15	1	2								
51	4	70-71	432	432.7	432.71	F	M	300		12				1					
51	6	70-71	435	436.9	436.91	C-F	G	302	15	10	1								
51	7	56-57	436.2	436.76	436.77	C	M	305	14	1			1	1					
52	3	75-76	440.1	440.85	440.86	C	G	301	18				1	7	1				
52	5	68-69	443.1	443.78	443.79	A	G	306	10				1		2				
52	6	71-72	444.6	445.31	445.32	C	G	311	10				1		1				
53	1	105-106	446.7	447.75	447.76	C	P	308	8				1						
53	2	75-76	448.2	448.95	448.96	A	M-P	303	16	1			2		1	1			
53	4	75-76	451.2	451.95	451.96	A	P	304	8				1						
53	6	76-77	454.17	454.93	454.94	F	G	300	15										
54	3	99-100	459.3	460.29	460.3	C	G	300	18			4		1					
54	4	41-42	460.8	461.21	461.22	C	M	302	14			2							
54	5	100-101	462.3	463.3	463.31	C	M	300	22	1			2	1	2			4	
55	1	102-103	465.9	466.92	466.93	C	M	304	16				3	2	3				
55	2	72-73	467.4	468.12	468.13	C	G	303	16				6		4				
55	CC	6-7	469.84	469.9	469.91	C	G	304	15				5		8				
56	2	75-76	477	477.75	477.76	C	M-P	301	13				3		18				
56	4	74-75	480	480.74	480.75	A	P	303	16	1			4	2		1			
56	6	79-80	483	483.79	483.8	C	M	302	11						1				
57	2	72-73	486.6	487.32	487.33	C	G	301	11						1				
57	4	80-81	489.6	490.4	490.41	A	M	305	10				2	2	1				
58	3	80-81	496.42	497.22	497.23	C	G	301	11				5	7			1		
58	5	75-76	499.42	500.17	500.18	C	M	303	13					7					
58	7	75-76	502.42	503.17	503.18	C	G-M	303	10				1		13			2	
59	2	60-61	505.8	506.4	506.41	C	G	301	12						15				
61	2	46-47	524.96	524.97	C	M	305	14				3		13					
62	2	72-73	534.6	535.32	535.33	C	G	300	18				9				3		

Table 4 - continued

Core	Section	Sample Interval	Core Top Depth (mbsf)	Sample Top Depth (mbsf) CSF-A	Sample Bottom Depth (mbsf) CSF-A	Nanno Abundance	Preservation	Total Abundance	Diversity	<i>Pseudodemiania ovata</i>	<i>Pseudomiliania pacifica</i>	<i>Reticulofenestra amplis</i>	<i>Reticulofenestra asanoi</i>	<i>Reticulofenestra daviesi</i>	<i>Reticulofenestra dicyoda</i>	<i>Reticulofenestra filewiczi</i>	<i>Reticulofenestra gelida</i>	<i>Reticulofenestra haqii</i> (3-5)	<i>Reticulofenestra minuta</i>
44	2	85-86	361.9	362.75	362.76	C	G	300	19	31							13	19	3
44	4	75-76	364.9	365.65	365.66	C	G	305	16								4	57	
44	6	75-76	367.9	368.65	368.66	C	G	301	20	26						1	23	3	
45	2	76-77	371.5	372.26	372.27	C	M	302	16	5						2	5	2	
45	4	75-76	374.5	375.25	375.26	A	G	302	16	1						3	2		
45	6	75-76	377.5	378.25	378.26	A	G	303	15							1	2	2	
46	4	69-70	384.08	384.77	384.78	C	G-M	308	19	3						1	1	28	
46	6	67-68	387.08	387.75	387.76	F	G	306	23		11				12	1	4	6	2
47	1	74-75	389.2	389.94	389.95	C	M-G	302	18	5		2			10	P	7		
47	4	78-79	393.7	394.48	394.49	C	G	303	17							7	3	3	
47	6	84-85	396.7	397.54	397.55	C	G	303	19	6						2	8	2	
48	2	71-72	400.2	400.91	400.92	C	G-M	302	21	2		2				1	2	1	
48	4	71-72	403.2	403.91	403.92	F	G	302	20	7							10	2	
48	6	71-72	406.2	406.91	406.92	C	G	304	15	9							10	9	1
49	3	75-76	411.3	412.05	412.06	A	G	306	19	5	1							3	
50	2	75-76	419.4	420.15	420.16	C	G	300	16		1				1		25	5	
50	4	75-76	422.4	423.15	423.16	A	P	302	14										
50	6	75-76	425.4	426.15	426.16	A	M	322	11									8	
51	2	70-71	429	429.7	429.71	C	G	301	15								1	6	
51	4	70-71	432	432.7	432.71	F	M	300	12							5		4	4
51	6	70-71	435	436.9	436.91	C-F	G	302	15								2	1	
51	7	56-57	436.2	436.76	436.77	C	M	305	14							1		6	7
52	3	75-76	440.1	440.85	440.86	C	G	301	18	1	1				6	1	1	3	
52	5	68-69	443.1	443.78	443.79	A	G	306	10									1	
52	6	71-72	444.6	445.31	445.32	C	G	311	10							1	2		
53	1	105-106	446.7	447.75	447.76	C	P	308	8						1				
53	2	75-76	448.2	448.95	448.96	A	M-P	303	16						1		10	1	
53	4	75-76	451.2	451.95	451.96	A	P	304	8										
53	6	76-77	454.17	454.93	454.94	F	G	300	15						1		3	7	9
54	3	99-100	459.3	460.29	460.3	C	G	300	18			1	1		1	1	5	6	
54	4	41-42	460.8	461.21	461.22	C	M	302	14				4		1	1	10	29	2
54	5	100-101	462.3	463.3	463.31	C	M	300	22	1	1				7	1	32	45	
55	1	102-103	465.9	466.92	466.93	C	M	304	16	1	2				3	3	18	23	
55	2	72-73	467.4	468.12	468.13	C	G	303	16		1				1	1	9	8	
55	CC	6-7	469.84	469.9	469.91	C	G	304	15				2		2	1	19	2	
56	2	75-76	477	477.75	477.76	C	M-P	301	13								33	1	
56	4	74-75	480	480.74	480.75	A	P	303	16						7		2	2	
56	6	79-80	483	483.79	483.8	C	M	302	11		3				1		28	1	
57	2	72-73	486.6	487.32	487.33	C	G	301	11		1				1			4	
57	4	80-81	489.6	490.4	490.41	A	M	305	10				2						
58	3	80-81	496.42	497.22	497.23	C	G	301	11				3		1	4	3		
58	5	75-76	499.42	500.17	500.18	C	M	303	13		1				5		1	3	
58	7	75-76	502.42	503.17	503.18	C	G-M	303	10						2			3	
59	2	60-61	505.8	506.4	506.41	C	G	301	12						2		4	3	
61	2	46-47	524.96	524.97	C	M	305	14									12	5	1
62	2	72-73	534.6	535.32	535.33	C	G	300	18		13				27	1	13	43	10

Table 4 - continued

Core	Section	Sample Interval	Core Top Depth (mbsf)	Sample Top Depth (mbsf) CSF-A	Sample Bottom Depth (mbsf) CSF-A	C Nanno Abundance	G Preservation	Total Abundance	Diversity	Reticulofenestra minutula		
44	2	85-86	361.9	362.75	362.76	C	G	300	19			29
44	4	75-76	364.9	365.65	365.66	C	G	305	16	27		25
44	6	75-76	367.9	368.65	368.66	C	G	301	20	3		27
45	2	76-77	371.5	372.26	372.27	C	M	302	16	2		63
45	4	75-76	374.5	375.25	375.26	A	G	302	16			22
45	6	75-76	377.5	378.25	378.26	A	G	303	15			21
46	4	69-70	384.08	384.77	384.78	C	G-M	308	19			39
46	6	67-68	387.08	387.75	387.76	F	G	306	23	4		37
47	1	74-75	389.2	389.94	389.95	C	M-G	302	18	10		21
47	4	78-79	393.7	394.48	394.49	C	G	303	17	1		23
47	6	84-85	396.7	397.54	397.55	C	G	303	19		1	44
48	2	71-72	400.2	400.91	400.92	C	G-M	302	21	1		34
48	4	71-72	403.2	403.91	403.92	F	G	302	20	1		55
48	6	71-72	406.2	406.91	406.92	C	G	304	15			28
49	3	75-76	411.3	412.05	412.06	A	G	306	19			21
50	2	75-76	419.4	420.15	420.16	C	G	300	16	1		47
50	4	75-76	422.4	423.15	423.16	A	P	302	14			31
50	6	75-76	425.4	426.15	426.16	A	M	322	11	6		9
51	2	70-71	429	429.7	429.71	C	G	301	15	1		33
51	4	70-71	432	432.7	432.71	F	M	300	12	4		49
51	6	70-71	435	436.9	436.91	C-F	G	302	15	2		27
51	7	56-57	436.2	436.76	436.77	C	M	305	14	2		32
52	3	75-76	440.1	440.85	440.86	C	G	301	18			38
52	5	68-69	443.1	443.78	443.79	A	G	306	10	1		8
52	6	71-72	444.6	445.31	445.32	C	G	311	10			11
53	1	105-106	446.7	447.75	447.76	C	P	308	8			18
53	2	75-76	448.2	448.95	448.96	A	M-P	303	16			12
53	4	75-76	451.2	451.95	451.96	A	P	304	8	1		20
53	6	76-77	454.17	454.93	454.94	F	G	300	15	4		51
54	3	99-100	459.3	460.29	460.3	C	G	300	18	2		48
54	4	41-42	460.8	461.21	461.22	C	M	302	14	3		20
54	5	100-101	462.3	463.3	463.31	C	M	300	22	1		91
55	1	102-103	465.9	466.92	466.93	C	M	304	16	2		36
55	2	72-73	467.4	468.12	468.13	C	G	303	16	10		40
55	CC	6-7	469.84	469.9	469.91	C	G	304	15			50
56	2	75-76	477	477.75	477.76	C	M-P	301	13	2		48
56	4	74-75	480	480.74	480.75	A	P	303	16	1		18
56	6	79-80	483	483.79	483.8	C	M	302	11	28	1	57
57	2	72-73	486.6	487.32	487.33	C	G	301	11	1		18
57	4	80-81	489.6	490.4	490.41	A	M	305	10			6
58	3	80-81	496.42	497.22	497.23	C	G	301	11			36
58	5	75-76	499.42	500.17	500.18	C	M	303	13	2		31
58	7	75-76	502.42	503.17	503.18	C	G-M	303	10			27
59	2	60-61	505.8	506.4	506.41	C	G	301	12			39
61	2	46-47	43	524.96	524.97	C	M	305	14		1	43
62	2	72-73	534.6	535.32	535.33	C	G	300	18	1	1	38

APPENDIX C

FIGURES

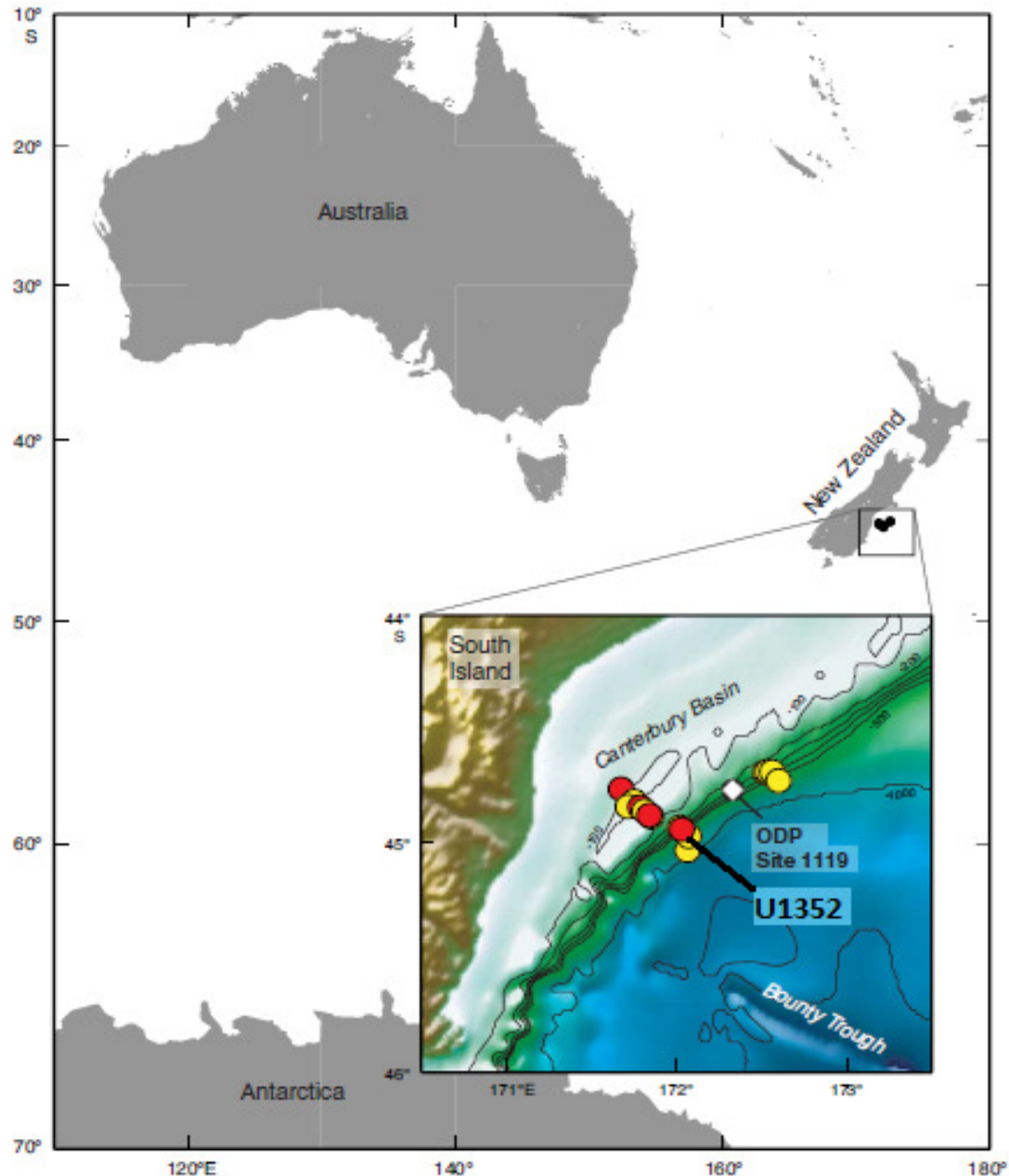


Figure 1: Map of Canterbury Basin on the eastern margin of South Island, New Zealand. Primary drilling sites are indicated in red, secondary drilling sites are indicated in yellow (modified from Shipboard Scientific Party, 2010).

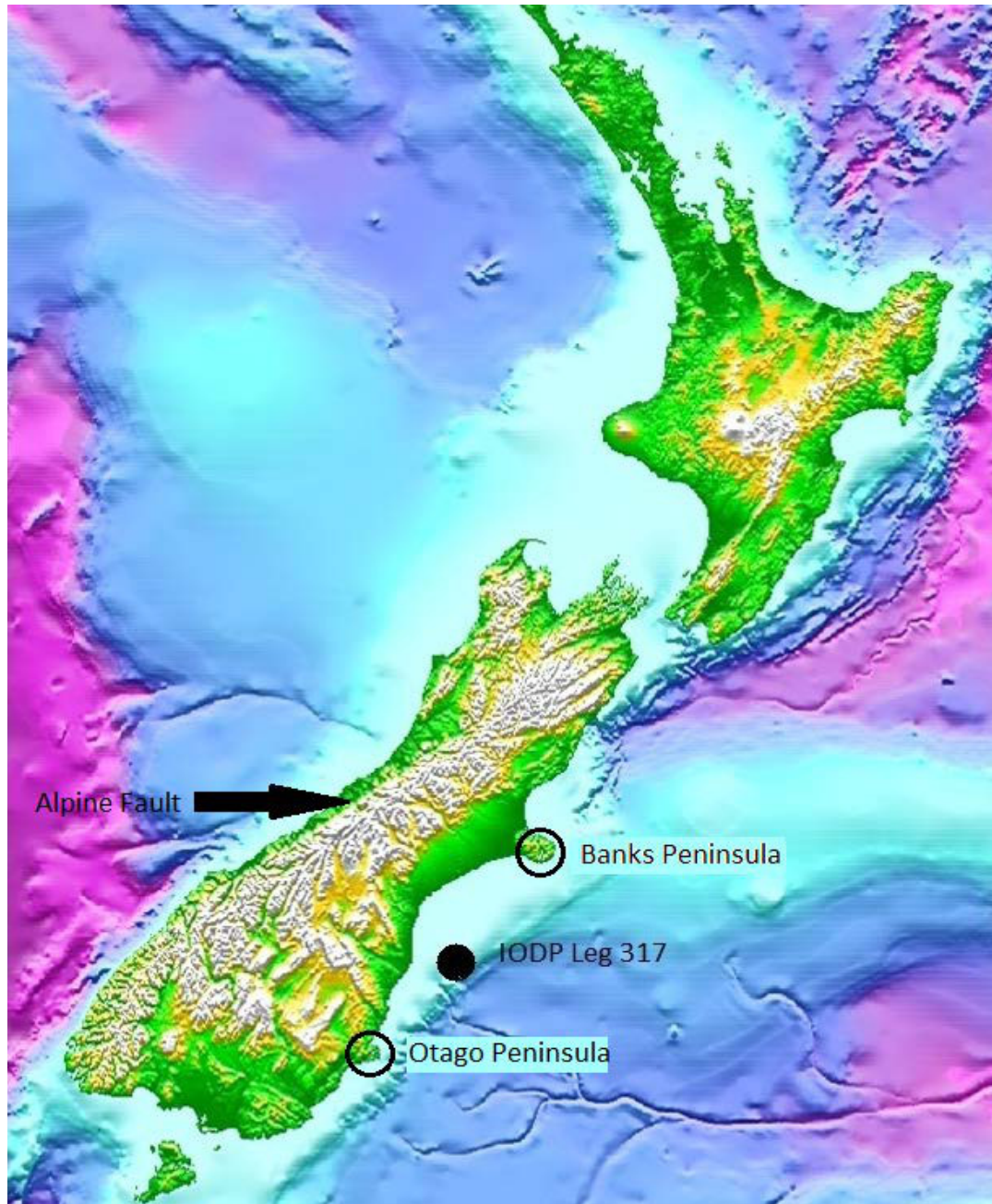


Figure 2: Regional Map of New Zealand including the Otago and Banks Peninsulas (mid-Miocene volcanic centers) and Alpine Fault.

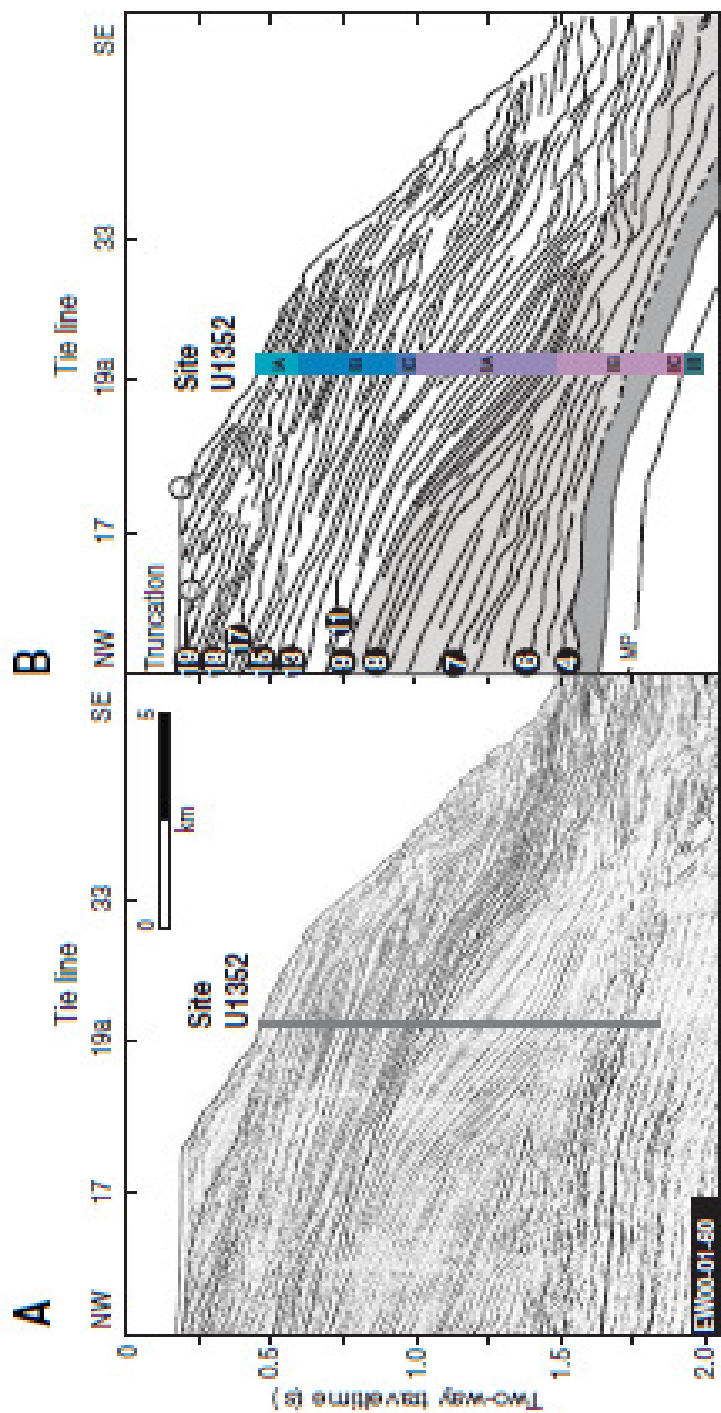


Figure 3: Correlation of lithologic units defined at slope Site U1352 an interpreted dip-oriented seismic profile. **A.** Uninterpreted profile showing site location. **B.** Sequence boundary interpretation (Shipboard Scientific Party, 2010).

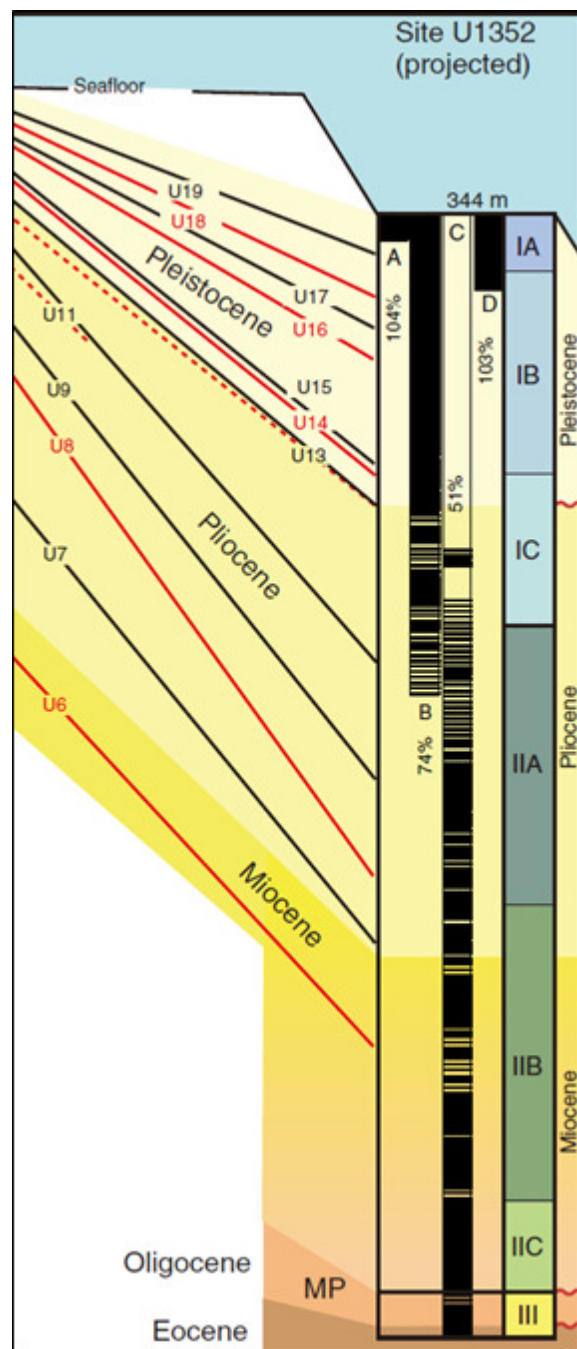


Figure 4: Summary of core recovery at Site U1352. MP = Marshall Paraconformity (modified from Shipboard Scientific Party, 2010).

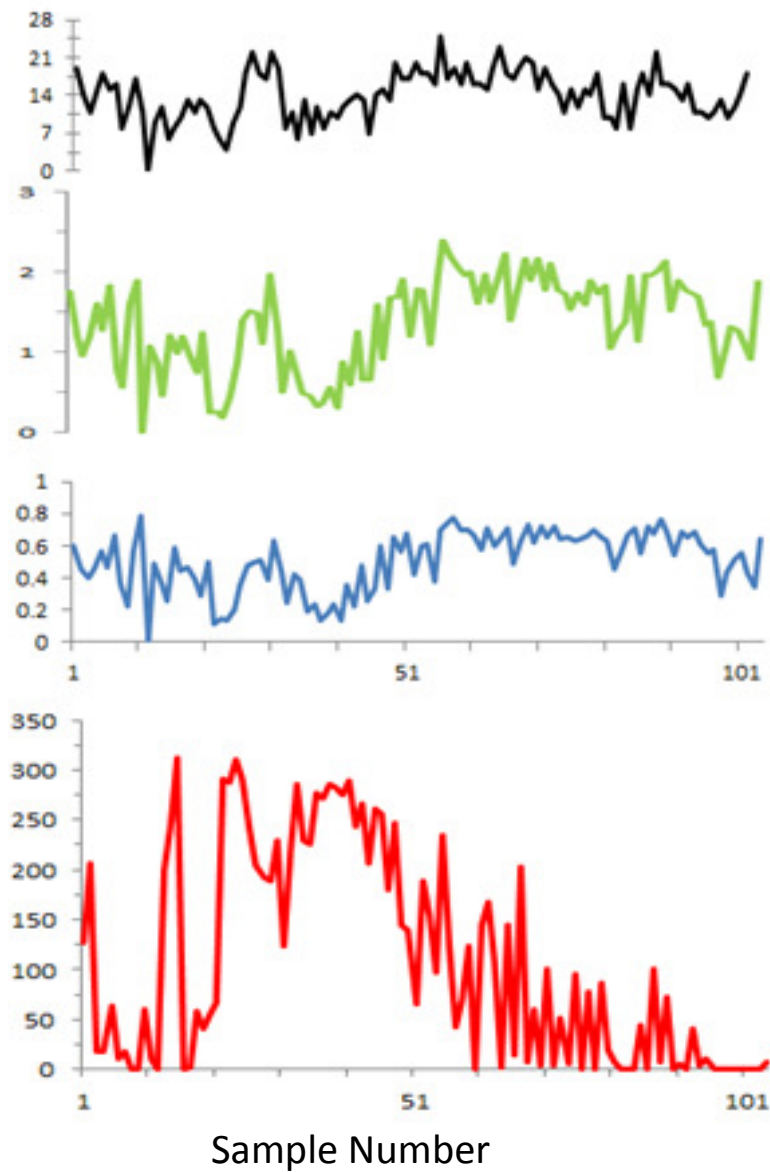


Figure 5: Line graph displaying inverse relationship between Hole U1352B species richness, evenness, Shannon Diversity and abundance of *Gephyrocapsa aperta*. **GREEN** delineates Shannon diversity indices values, the **BLACK** graph shows species richness, species evenness is plotted in **BLUE**, and the **RED** line graph represents *G. aperta* abundance.

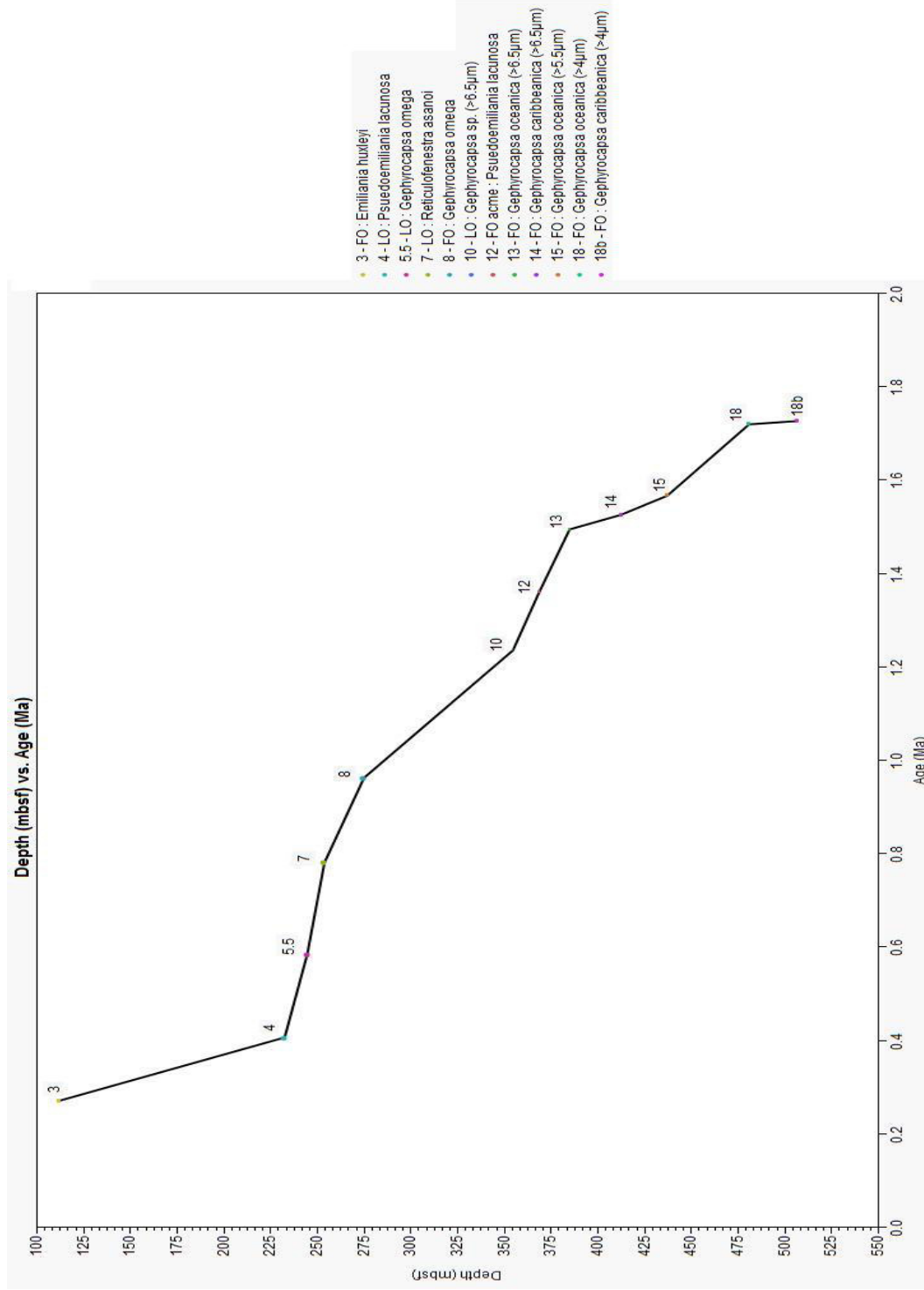


Figure 6: Age vs. Depth Plot of observed calcareous nannofossil datums from Hole U1352B

APPENDIX D

PLATES

Plate 1: Pleistocene nannofossils from the Canterbury Basin, Hole U1352B. **1, 2.** *Cyclicargolithus floridanus*. **3, 4.** *Calcidiscus leptoporus*. **5, 6.** *Coccolithus pelagicus*. **7, 8.** *Coccolithus pelagicus* f. *braarudii*. **9, 10.** *Emiliania huxleyi*. **11, 12.** *Gephyrocapsa aperta*. **13, 14.** *Gephyrocapsa caribbeonica* (3-4 μm). **15, 16.** *Gephyrocapsa caribbeonica* (>6.5 μm). **17, 18.** *Gephyrocapsa caribbeonica* (4-5.5 μm).

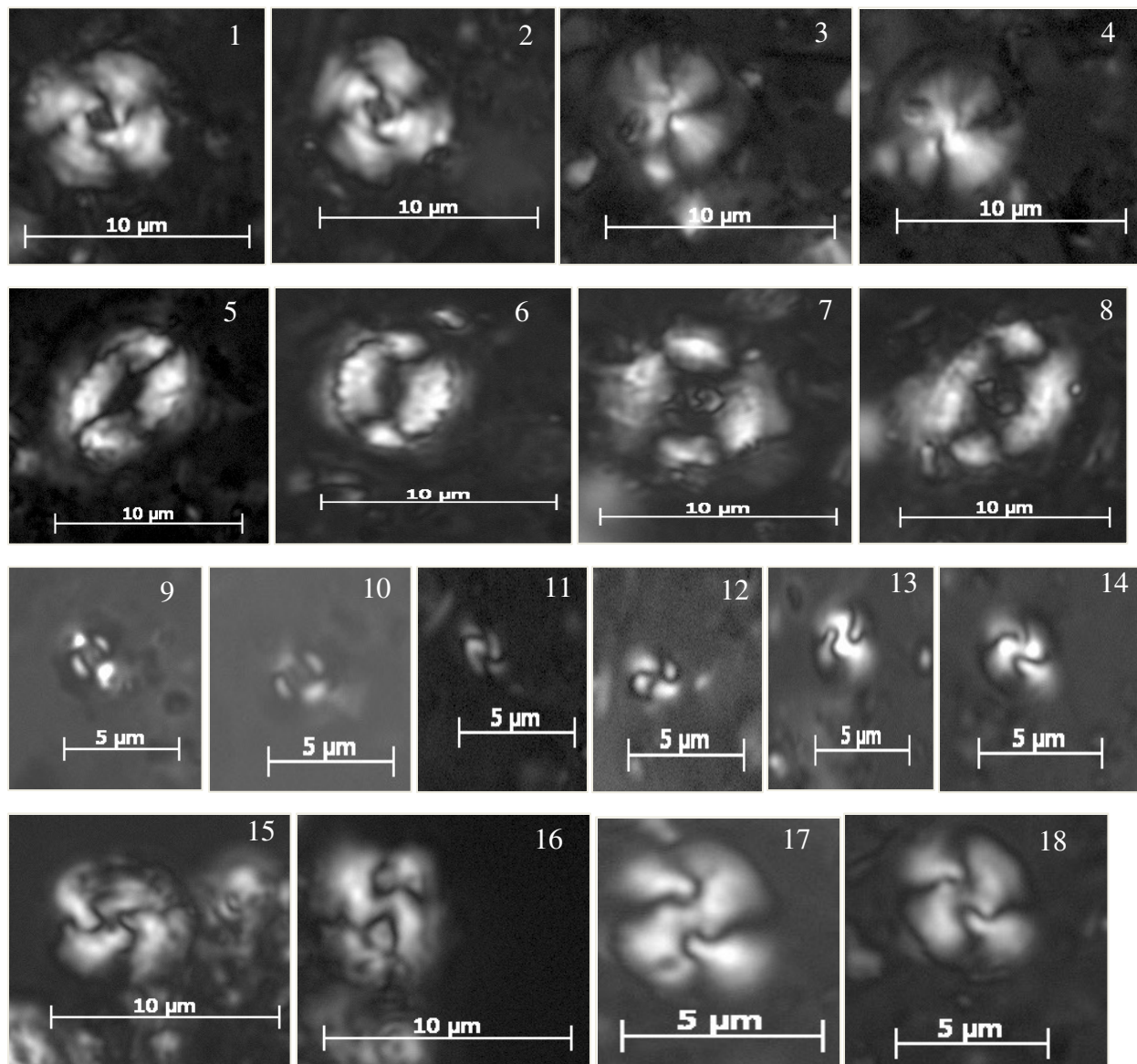
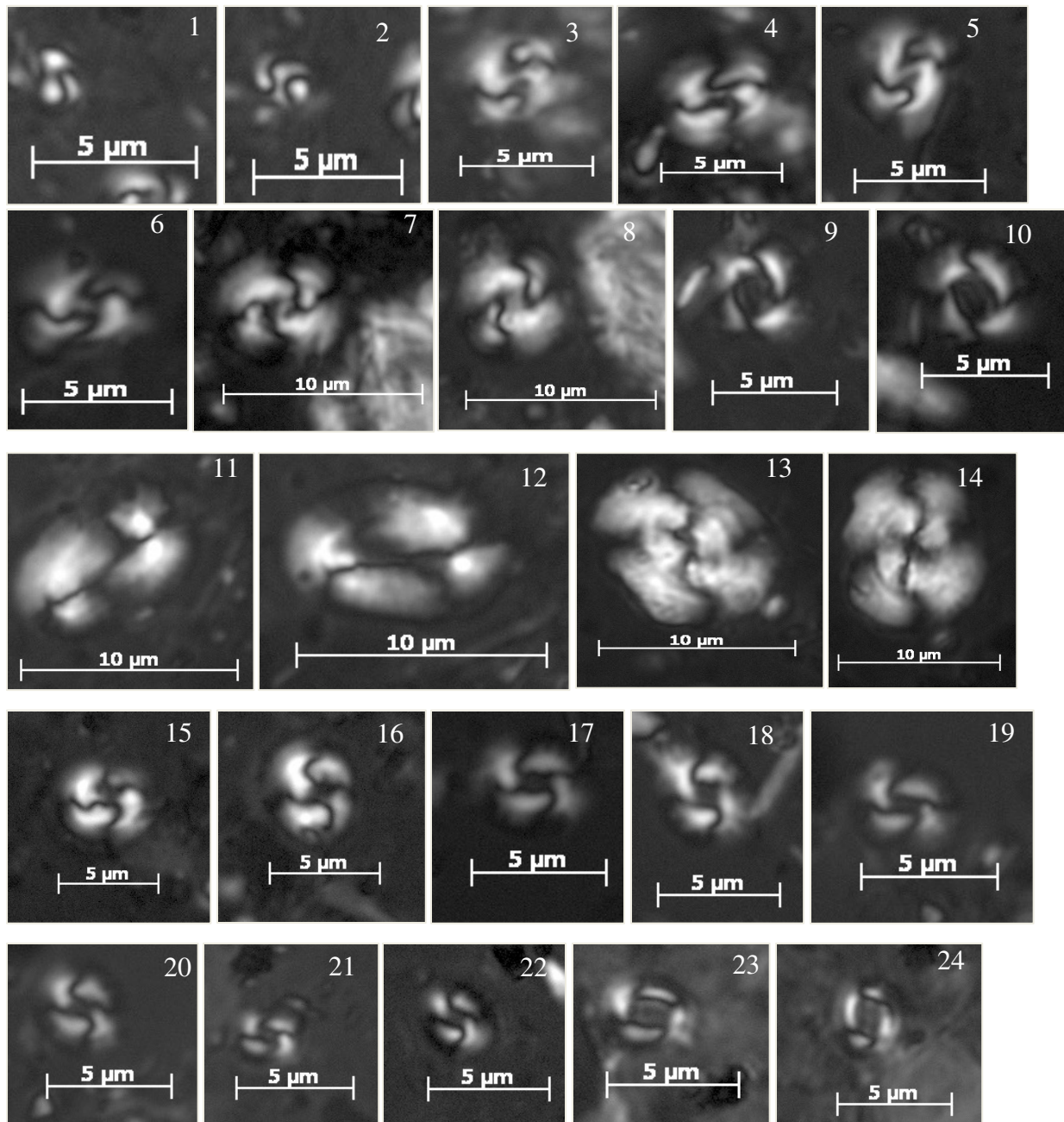


Plate 2: 1, 2. *Gephyrocapsa crassipons*. 3, 4. *Gephyrocapsa oceanica* (>5.5 μm). 5, 6. *Gephyrocapsa oceanica* (4-5.5 μm). 7, 8. *Gephyrocapsa oceanica* (>6.5 μm). 9, 10. *Pseudoemiliania lacunosa*. 11, 12. *Helicosphaera carteri*. 13, 14. *Dictyococcites bisecta*. 15, 16. *Reticulofenestra dictyoda*. 17, 18. *Reticulofenestra haqii* (3-5 μm). 19, 20. *Reticulofenestra haqii* (<3 μm). 21, 22. *Reticulofenestra minutula*. 23, 24. *Reticulofenestra minutula*



REFERENCES

- Adams, C.J.D., 1979. Age and origin of the Southern Alps. In Walcott, R.I., and Cresswell, M.M. (Eds.), *The Origin of the Southern Alps*. Roy. Soc. N. Z. Bulletin, 18:73–78.
- Batt, G.E., Braun, J., Kohn, B., and McDougall, I., 2000. Thermochronological analysis of the dynamics of the Southern Alps, New Zealand. *Geol. Soc. Am. Bull.*, 112(2):250–266.
- Billard, C., 1994. Life cycles, In Green, J.C. and Leadbeater, B.S.C. Eds, *The Haptophyte Algae*. The Syst. Asso. Spec. Vol. 51, Clarendon Press, Oxford, pp. 167-186.
- Bown, P.R. (Ed.), 1998. *Calcareous Nannofossil Biostratigraphy*: Dordrecht, The Netherlands (Kluwer Academic Publ.).
- Bramlette, M.N., and Riedel, W.R., 1954. Stratigraphic value of the discoasters and some other microfossils related to recent coccolithophores. *Jour. Pal.*, 28:385-403.
- Bramlette, M.N., and Wilcoxon, J.A., 1967. Middle Tertiary calcareous nannoplankton of the Cipero Section, Trinidad. *Tul. Stud. Geo.*, 5:93-131.
- Browne, G.H., and Field, B.D., 1988. *A review of Cretaceous–Cenozoic sedimentation and tectonics, east coast, South Island, New Zealand*. In James, D.P., and Leckie, D.A. (Eds.), *Sequences, Stratigraphy, Sedimentology: Surface and Subsurface*. Can. Soc. Pet. Geol. Mem., 15:37–48.
- Bukry, D., 1973. Low-latitude coccolith biostratigraphic zonation. In Edgar, N.T., Saunders, J.B., et al, Init. Repts. DSDP: Washington (U.S. Govt. Printing Office). 15:685-703.
- Bukry, D., and Percival, S.F., 1971. New Tertiary calcareous nannofossils. *Tul. Stud. Geol. and Paleo.*, 8:123-146.
- Carter, R.M., and Landis, C.A., 1972. Correlative Oligocene unconformities in southern Australasia. *Nature (London), Phys. Sci.*, 237:12–13.
- Carter, R.M., McCave, I.N., and Carter, L., 2004a. Leg 181 synthesis: Fronts, flows, drifts, volcanoes, and the evolution of the southwestern gateway to the Pacific Ocean, Eastern New Zealand. In Richter, C. (Ed.), *Proc. ODP Sci. Results*, 181, College Station, TX (Ocean Drilling Program) 1-112.
- Carter, R.M., McCave, I.N., and Carter, L., 2004b. Leg 181 synthesis: fronts, flows, drifts, volcanoes, and the evolution of the southwestern gateway to the Pacific Ocean, eastern New Zealand. In Richter, C. (Ed.), *Proc. ODP, Sci. Results*, 181: College Station, TX (Ocean Drilling Program), 1–112.

- Carter, R.M., and Norris, R.J., 1976. Cenozoic history of southern New Zealand: an accord between geological observations and plate-tectonic predictions. *Earth Planet. Sci. Lett.*, 31(1):85–94.
- Carter, R.M., 1985. The mid-Oligocene Marshall Paraconformity, New Zealand: Coincidence with global eustatic sea-level fall or rise?. *J. Geol.*, 93(3):359–371.
- Carter, R.M., 1988. Post-breakup stratigraphy of the Kaikoura Synthem (Cretaceous–Cenozoic), continental margin, southeastern New Zealand. *N. Z. J. Geol. Geophys.*, 31:405–429.
- Carter, R.M., 2007. The role of intermediate currents in continental shelf-slope accretion: Canterbury Drifts, SW Pacific Ocean. In Viana, A.R., and Rebesco, M. (Eds.), *Economic and Paleoceanographic Significance of Contourite Deposits*. Geol. Soc. Spec. Publ., 276(1):129–154
- De Kaenel, E., Siesser, W.G., and Murat, A., 1999. Pleistocene calcareous nannofossil biostratigraphy and the western Mediterranean sapropels, Sites 974 to 977 and 979. In Zahn, R. et al. (Eds) *Proc. ODP, Sci. Results*, 161: College Station, TX (Ocean Drilling Program), 159-183.
- Field, B.D., and Browne, G.H., 1989. Cretaceous and Cenozoic Sedimentary Basins and Geological Evolution of Canterbury Region, South Island, New Zealand. *N. Z. Geol. Surv.*, 2.
- Fleming, C.A., 1962. New Zealand biogeography: a paleontologist's approach. *Tuatara*, 10:53–108.
- Fulthorpe, C.S., Carter, R.M., Miller, K.G., and Wilson, J., 1996. Marshall paraconformity: a mid-Oligocene record of inception of the Antarctic Circumpolar Current and coeval glacio-eustatic lowstand? *Mar. Pet. Geol.*, 13(1):61–77.
- Fulthorpe, C.S., and Carter, R.M., 1991. Continental-shelf progradation by sediment-drift accretion. *Geol. Soc. Am. Bull.*, 103(2):300–309.
- Gartner, S. and Bukry, D., 1969. Tertiary holococcoliths. *J. Paleo.*, 43:1213-1221.
- Gartner, S., 1977. Calcareous nannofossil biostratigraphy and revised zonation of the Pleistocene. *Mar. Micropaleo.*, 2:1-25.
- Hay, W.W., Mohler, H.P., Roth, P.H., Schmidt, R.R., and Bourdreaux, J.E., 1967. Calcareous nannoplankton zonation of the Cenozoic of the Gulf Coast and Caribbean-Antillean area and transoceanic correlation. *Trans. Gulf Coast Asso. Geol. Soc.*, 17:428-480.
- Honjo, S., 1976. Coccoliths: Production, Transportation and Sedimentation. *Mar. Micropaleo.*, 1:65-79.

- Inouye, A. and M. Kawachi., 1994. The haptoneema. In Green, J.C. and Leadbeater, B.S.C. (Eds.), *The Haptophyte Algae* The Syst. Asso. Spec. Vol. 51, Clarendon Press, Oxford, 73-89.
- Isenberg, H.D., Douglas, S.D., Lavine, L.S., and Weissfellner, H., 1967. Laboratory studies with coccolithophorid calcification. *Int. Conf. Trop. Ocean. Miami, Proc.*, 155-177
- Kamp, P.J.J., 1987. Age and origin of the New Zealand orocline in relation to alpine fault movement. *J. Geol. Soc. (London, U. K.)*, 144(4):641–652.
- King, P.R., 2000. Tectonic reconstructions of New Zealand: 40 Ma to the present. *N. Z. J. Geol. Geophys.*, 43:611–638.
- Lu, H., Fulthorpe, C.S., and Mann, P., 2003. Three-dimensional architecture of shelf-building sediment drifts in the offshore Canterbury Basin, New Zealand. *Mar. Geol.*, 193(1–2):19–47.
- Lu, H., Fulthorpe, C.S., Mann, P., and Kominz, M., 2005. Miocene–Recent tectonic and climate controls on sediment supply and sequence stratigraphy: Canterbury Basin, New Zealand. *Basin Res.*, 17(2):311–328.
- Manton, I. and G.F. Leedale, 1969. Observations on the microanatomy of *Coccolithus pelagicus* and *Cricosphaera carterae*, with special reference to the origin and nature of coccoliths and scales. *J. Mar. Bio. Asso. UK*, 49:1-16.
- Martini, E., 1971. Standard Tertiary and Quaternary calcareous nannoplankton zonation. In Farinacci, A. (Ed.), *Proc. Int. Conf. Planktonic Microfossils*, 2:739–785.
- Molnar, P., Atwater, T., Mammerickx, J., and Smith, S., 1975. Magnetic anomalies, bathymetry and the tectonic evolution of the South Pacific since the Late Cretaceous. *Geophys. J. R. Astron. Soc.*, 40:383–420.
- Norris, R.J., Carter, R.M., and Turnbull, I.M., 1978. Cenozoic sedimentation in basins adjacent to a major continental transform boundary in southern New Zealand. *J. Geol. Soc. (London, U. K.)*, 135(2):191–205.
- Okada, H., and Bukry, D., 1980. Supplementary modification and introduction of code numbers to the low-latitude coccolith biostratigraphic zonation. (Bukry 1973, 1975), *Mar. Micropaleo.*, 5, 321-325.
- Pienaar, R.N., 1994. Ultrastructure and calcification of coccolithophores. In: Winter, A. and Siesser, W.G. (Eds), *Coccolithophores*. Cambridge University Press, Cambridge, 13-37.
- Perch-Nielsen, K., 1985. Cenozoic calcareous nannofossils. In Bolli, H.M., Saunders, J.B., and Perch-Nielsen, K. (Eds.), *Plankton Stratigraphy*, Cambridge (Cambridge Univ. Press), 427-554.

- Roth, P.H., 1978. Cretaceous nannoplankton biostratigraphy and oceanography of the northwestern Atlantic Ocean. In: Benson, W.E., Sheridan, R.E., et al. (Eds.), *Init Rept. DSDP*. Washington (U.S. Govt Printing Office), 44:731-760.
- Rowson, J.D., Leadbeater, B.S.C. and Green, J.C., 1986. Calcium carbonate deposition in the motile (*Crystallithus*) phase of *Coccolithus pelagicus* (Prymnesiophyceae). *Br. Phy. Jour.*, 21:359-370.
- Shipboard Scientific Party, 2010. Canterbury Basin Sea Level: Global and local controls on continental margin stratigraphy. *IODP Prel. Rept.*, 317.
- Siesser, W.G. and Winter, A., 1994. Composition and morphology of coccolithophore skeletons. In: Winter, A. and Siesser, W.G. (Eds), *Coccolithophores*. Cambridge University Press, Cambridge, 51-62.
- Sissingh, W., 1977. Biostratigraphy of Cretaceous calcareous nannoplankton. *Geologie en Mijnbouw*, 56: 37-65.
- Takayama and Sato, 1987. Coccolith Biostratigraphy of the North Atlantic Ocean, Deep Sea Drilling Project Leg 94. In: Ruddiman, W. F., Kidd, R. B., Thomas, E., et al. (Eds), *Init. Rept. DSDP*. 19. Washington (U.S. Govt. Printing Office) 94:651-702.
- Tippett, J.M., and Kamp, P.J.J., 1993a. Fission track analysis of the late Cenozoic vertical kinematics of continental Pacific crust, South Island, New Zealand. *J. Geo. Res.*, 98(9):16119–16148.
- Tippett, J.M., and Kamp, P.J.J., 1993b. The role of faulting in rock uplift in the Southern Alps, New Zealand. *N. Z. J. Geol. Geophys.*, 36(4):497–504
- Wellman, H.W., 1971. Age of the Alpine Fault, New Zealand. *Proc. Int. Geo. Cong.*, 22nd, 4:148–162.
- Wise, S.W., 1982. Calcareous nannofossils: An update. *Third North American Paleontological Convention, Proceedings* 2:588a-588j.

BIOGRAPHICAL SKETCH

Birth date and Place:

September 28, 1986 in West Palm Beach, FL

Education:

Masters of Science in Geology, Florida State University (05/03/2013)

Bachelors of Science in Geology, Florida State University (08/08/2009)

Academic Experience:

Calcareous Nannofossil Lab, Florida State University

Research Assistant

June 2012 - Present

- Field work on *R/V Bellows* and *R/V Weatherbird II* in the Gulf of Mexico obtaining modern nannoplankton samples for Dr. Sherwood Wise's research project looking into the effects of the 2010 BP oil spill on calcareous nannoplankton assemblages.
- Preparation and analysis of nannoplankton samples using Scanning Electron Microscopy
- Training new research assistants in proper sampling, SEM prep, and SEM analysis of Gulf of Mexico nannoplankton samples.

Antarctic Marine Geology Research Facility, Tallahassee FL

Research Assistant/

August 2009 – June 2012/

Laboratory Assistant

July 2007 –August 2009

- Cutting, splitting and describing sediment cores taken from both on the Antarctic continent and offshore.
 - Core Descriptions include both macro and micro analysis for mineralogical and paleontological components as well as grain size. Descriptions are converted into digital format using Adobe Illustrator and included in a published log of all cores taken during a research cruise.
- Core imaging and X-ray photography
- Scientific sampling of sediment cores for Antarctic scientists worldwide.
- Assist in duties of properly maintaining and curating the AMGRF's collection of sediment cores, rock samples, grab samples, seafloor photographs, etc.

Paleontology Lab, Florida State University

Laboratory Assistant

January 2009 – April 2009

- Curation of the paleontology collection housed in the Department of Geological Sciences' Paleontology Lab

Calcareous Nannofossil Lab, Florida State University

Laboratory Assistant

May 2007 – July 2007

- Preparation of sediment samples for Dr. Denise Kulhanek, during her doctoral research at FSU

Professional Experience:

BugWare, Inc., Tallahassee, FL.

Paleontology Technician

August 2011

- On-site preparation of drill cutting samples as smear slides for analysis by nannofossil paleontologists stationed on petroleum exploration rigs in the Gulf of Mexico.

Professional Affiliations:

- American Association of Petroleum Geologists (Student Member)
- Geological Society of America (Student Member)
- Society for Sedimentary Geology (Student Member)
- International Nannoplankton Association (Student Member)

Affiliated Projects:

- After-the-fact estimations of the calcareous nannoplankton composition and quantity present during the 2010 Macondo oil spill in the NE Gulf of Mexico: A work in progress.
 - Authors: Agbali, Aisha E.; Cruz, Jarrett W.; Flower, Benjamin P.; Foley, Susan M.; Hollander, David; Jeffrey, Wade H.; Myers, Nicholas R.; Nienow, James A.; Snyder, Richard A.; and Wise, Sherwood W. Jr.
- Descriptions of Sediment Recovered by the R/V *Nathaniel B. Palmer*, United States Antarctic Program: Cruise 7, 2001.
<http://arf.fsu.edu/publications/documents/NBP01-07.pdf>
- Descriptions of Sediment Recovered by the R/V *Nathaniel B. Palmer*, United States Antarctic Program: Cruise 1, 2000
http://arf.fsu.edu/publications/documents/NBP_2000_01.pdf